

# ***Interactive comment on “Modelling the effects of ice transport and sediment sources on the form of detrital thermochronological age probability distributions from glacial settings” by Maxime Bernard et al.***

**Response to the reviewer.**

**We first wish to particularly thanks the Pr. Ehlers for his review of the paper. His comments are very relevant and have been very appreciated by the authors.**

**We took into consideration all the comments and we present our reply point by point.**

**GENERAL COMMENTS:**

*G1. The general validity (beyond the simulations presented) of the authors results and interpretations is difficult to assess. If I understand the text and Table 1 correctly, the authors present a set of simulations with only one set of parameters. These results are nicely presented and described, but the primary interpretations of the paper (e.g. 1,500 yr equilibrium time for observed age-distributions; sediment trapping in tributary glaciers, hill slope vs. Glacial contributions to observed age distributions) are based on this single (?) set of chosen parameters. The results would be generalisable and more broadly applicable if a small set of additional simulations with a sensitivity analysis were included. For example, picking the least well constrained climate, ice, and hill slope parameters and picking reasonable values above and below what is shown in Table 1 should be considered to evaluate how robust the interpretations are in the text. I suggest these additional figures be shown in the supplementary material and then referred to in the main text, or highlighted in a new discussion section with a new figure that compare results.*

In the initial version of the study we presented the models with only one set of parameters for the simulated glacier dynamics. We share the concern of the Pr. Ehlers, so we performed a set of additional simulations with a set of parameter values that lead to a glacier size ~1000 m longer and shorter than the modelled glacier presented in the main study. We chose this range of glacier size difference because greater discrepancies would lead to very different glaciers dynamics and glacier thickness compared to the ITMIX experiments results, which is our calibration for the Tiedemann glacier. The additional models are now presented in a dedicated section in the supplementary materials, where we compare the results with the reference model (i.e. presented in the main text). Overall, the resulting detrital age distributions and equilibrium time for the frontal moraine of these additional models do not significantly vary from the reference model.

*G2. The results of Enkelmann and Ehlers (2015, Chem Geo) compared AFT ages across the ice cored moraine, outwash, and older moraines in front of the modern glacial terminus. The ice cored moraine and outwash samples were statistical identical (Fig. 6E), meaning that multiple ice cored samples when combined produce the same grain-age distribution as outwash. “slight differences” were observed between the individual ice cored moraine material in this study (Fig. 4 of Enkelmann and Ehlers). While the authors of this study (Bernard et al) explicitly say they are not trying to match observations in their study, in the discussion section they end making statements that do compare / evaluate the observations. There are suggested revisions related to this:*

*G2-a. In the start of the paper when describing the previous observational studies in the area (and the bedrock data you use), please add text that makes it clearer how these data were collected and which data sets are or are not relevant to how the model is setup and why. For example, the Enkelmann and Ehlers 2015 data are well suited for comparison to the model results (they come from ice cored moraine material at the end of the glacier). In contrast - the Ehlers et al. 2015 data are from glacial outwash and are not suitable for comparison to how the model is setup. The modelling*

*approach does not track particles through the subglacial hydrologic system. No comparisons to this later study should be made in this manuscript.*

*G2-b. The concluding discussion section (4.4) and Fig. 10 make model predictions that are more or less comparable to the observations of Enkelmann and Ehlers, 2015. Although some qualitative comparisons are made in the text, the manuscript would be much stronger if the data from Enkelmann and Ehlers, 2015 were also plotted in Fig. 10c and similarities / discrepancies are discussed.*

Initially, we did not aim to compare our results explicitly to the observations given that our synthetic steady Tiedemann glacier dynamics does not reflect the real Tiedemann glacier which is currently retreating. However, the comments of the two reviewers convinced us to consider such a comparison. As mentioned by the Pr. Ehlers, as our sediment particle sampling is focused on the frontal moraine, we only compare our results with the detrital age distributions from Enkelmann and Ehlers (2015) in which the samples come from the ice-cored terminal moraine. Such a comparison, with statistical tests, is presented in the revised version of the manuscript.

At the start of the paper we clarify the provenance of the samples from Enkelmann and Ehlers (2015) and Ehlers et al. (2015). We have also specified that we produced our bedrock ages according to the age-elevation from Enkelmann and Ehlers (2015) for the AFT data and from Ehlers et al. (2015) for the AHe data. In the revised version of the manuscript, the comparison of our detrital age distributions with the AFT data of the ice-cored terminal moraine samples from Enkelmann and Ehlers (2015) is made in section 4.4 (i.e. Implications for detrital sampling strategies) with the figure and the results from statistical tests presented in the Appendices. In that section we specified the provenance of the samples from Enkelmann and Ehlers (2015) (i.e. ice-cored terminal moraine).

*G3. The model setup and description needs to be clearer. It is not clear how erosion is done for hill slopes and how ages from hill slopes are mixed with the glacial sourced ages. It would greatly improve a readers understanding of this study if the coupling (and particle tracking) between hill slopes and glaciers was better explained, and also the sensitivity of their results (e.g. Fig. 7) to some of these parameters (e.g. see also comment G1 above). I also don't understand exactly how the 'uniform' erosion model was calculated with the ice model (see detailed comment below). The methods sections needs to explain the model setup for all this better. Section 2.1 (end) explains a non-linear diffusion model is used for hill slopes, but it's not described in enough detail how the sediment transport is done in this part of the landscape. The paper later on nicely explores how hill slope vs. Glacial sediment sources impact detrital cooling ages. Thus, some additional text in the methods section would make it much easier to understand the model results. As it's written now, I could not reproduce your results if I wanted to.*

We considered the comment of the Pr. Ehlers and have made the model setup and description clearer having entirely rewritten section 3. In the case of uniform erosion, we specified the production of particles in each cell of the model for both hillslope and glacial sources. In the case of non-uniform erosion (section 3.5), the erosion is determined by the erosion laws presented in section 2.1. The thermochronological age of a particle is based on the source location elevation of that particle and the appropriate age-elevation profile. Thus, each particle carries an age which is not modified during the particle transport. The mixing of particles (i.e. ages) is the result of the transport pattern. However, during the sampling process we can choose to identify and sample particles according to their source location (hillslopes or glaciers). The sensitivity of parameters for figure 7 are now presented in the supplementary materials.

A particle is formed once the erosion products in a cell reach a thickness threshold ( $H_s = 0.01\text{m}$ ). Then, each particle is transported away according to the transport laws for hillslopes (Eq. 8) and for ice (Eq. 9). This is now explained in the start of section 2.2.

*G4. Comparison of distributions should include statistical tests. Section 4.4 (see also detailed comment 26 below) presents an analysis of how representative point samples across a moraine compare to the mean of all samples and the bedrock distribution. This section is very useful for understanding how and where people could sample. However, the analysis does not statistically*

*evaluate if the different synthetically sampled distributions are the same or not. Visual / qualitative comparisons of distributions is dangerous, and I suspect (based on experience) that several of the distributions show in Fig. 10c will be statistically identical. If this section remains in the paper (which I hope it does), it's important the authors conduct a simple KS or Kuiper test to see if in fact the different distributions show in figure 10c are different or not. This comment could also potentially impact the conclusions presented in section 4.5. The text in section 4.4 and 4.5 is good, but simply needs support from a more quantitative comparison. Finally, as mentioned above for comment G2, this model result should be compared to observations that were collected from roughly this same area (Enkelmann and Ehlers, 2015).*

In the initial version of the manuscript, our comparative analysis was primarily qualitative as our goal is to describe the form of the detrital age distributions and link it to processes (i.e. sediment transport and erosion). In section 4.4, we compare the detrital age distributions over 4 regions within the frontal moraine to the catchment bedrock age distribution, and discussed the discrepancies that occur. The validity of statistical tests is not a given (e.g. Vermeesch, 2018), partly our concern regarding statistical tests. However, in the revised version of the manuscript we use two statistical tests (Kolmogorov-Smirnov and Kuiper tests) to compare our detrital age distributions with the catchment bedrock age distribution, and with the detrital age distributions from Enkelmann and Ehlers (2015). Given, this, we also highlight some contradictions between the inferences made from the two statistical tests.

*G5. The text is in general well written and clear. However, there are many small wording issues / grammatical problems throughout the text (e.g. missing articles, subject/ verb agreement) that are understandably hard to catch for a non-native speaker. I recommend a native speaker/co-author give the text another thorough read to correct these.*

We thank the Pr. Ehlers to have pointed out such wording and grammatical issues. We brought a particular attention to these issues in the revised version of the manuscript.

#### SPECIFIC COMMENTS:

0. *For clarity - all axis labels with 'Age' on them should say what age (e.g. "AFT Age") you are plotting since you work with two different systems in this study.*

Done.

1. *Abstract should make it clear if the langragian particle tracking is only for ice flow, or subglacial water.*

We now state in the new version of the manuscript (page 1 – line 15): “Sediments are tracked as Lagrangian particles formed by bedrock erosion, where their transport is restricted to ice or hillslope processes until they are deposited”.

2. *Page 2 paragraph starting at line 17: Also relevant to the content of this paragraph, and the study area investigated is the study by Yanites and Ehlers 2016 that documents how glacial sliding relates to bedrock thermochronometer ages (in a neighbouring valley in the Coast Mountains). Yanites, B. J. and Ehlers, T. A.: Intermittent glacial sliding velocities explain variations in long-timescale denudation, *Earth and Planetary Science Letters*, 450, 52–61, doi:10.1016/j.epsl.2016.06.022, 2016. Also - this manuscript is highly relevant to the following previous work and the authors should consider citing it in the introduction or discussion. Herman, F., et al., 2018. The response time of glacial erosion. *JGR - Earth Surface*. <https://doi.org/10.1002/2017JF004586>*

We thank the Pr. Ehlers for suggesting the studies relevant for our manuscript. We have added a small paragraph that mention the results of the study of Yanites and Ehlers 2016 (Page 2 -lines 20-24).

We also now mention the study of Herman et al. (2018) when we discuss the kinematics of our sediment transport model (Section 4.2) and the characteristic timescale for the glacier dynamics (Page 20 – lines 28-29).

3. *Page (pg) 3, line (ln) 12 - It might be worth clarifying here for readers that the Enkelmann and Ehlers 2015 studied sampled ICE across the ablation zone, and the Ehlers et al. 2015 study sampled glacial OUTWASH. This would help readers understand why you can not directly compare model predictions to one of these sets of observations..*

We have made this clear by modifying this sentence. (Page 3 – lines 16-19).

4. *Pg5, 6 model description. Hydrology effects on sliding are described here, but please also add a sentence or two that says if this is also included in the particle tracking for making SPDFs of cooling ages. Maybe you address this later.*

We have added the sentence “We stress again that we neglect the transport of particles by meltwater and focus only on the ice and hillslope processes.” (Page 7 – lines 22-23).

5. *Pg5, 6 - It is also important that this section says how you have calibrated the model for the subsurface hydrology. This aspect of the model is likely very important for how the data are interpreted, so some text on this aspect would be useful.*

We have added the sentence “We calibrated our hydrological model by a trial-error process by varying  $k_0$  (Eq.2) to lead to a reasonable value of basal ice sliding velocities (Table S1).” We have also added a short description in the supplementary material associated to Table S1 to show the parameters used for our calibration approach for the Tiedemann glacier. (Page 6 – lines 7-8, and Supplementary Table S1).

6. *Pg.6 - Your approach assumes all sediment comes from quarrying. I'm more or less ok with this (note fine sediment fractions were present in what we sampled for this glacier). However, please explain here if you account for the comminution (breaking down) of plucked material. Why could this be important? If 20x20cm rock is plucked in the upper reaches of the catchment it will break down during transport and provide fine grain material that was sampled. If a 20x20 cm rock is plucked from 100 m from the sample point - it wouldn't show up in sample. The material sampled for the Tiedemann glacier ice cored moraine and outwash was a 'bulk' sediment sample, but with nothing greater than 2x2cm size in it. I would be great if your modelling approach accounted for comminution, but I'm guessing this is not the case. So this effect needs to be acknowledged and the potential implications of it discussed in a model caveats section.*

We do not account for the comminution in our transport model as this would lead to computer-memory issues due to the too large number of particles tracked by the model. We have added a short paragraph to discuss the issue of such process in the sampling approach, in section 4.1 which deals with the limitations of our modelling approach (Page 20 – lines 12-15).

7. *Pg 6/7 - section 2.3. As indicated above, please explicitly state that water transport of detritus is not accounted for. Fluvial systems mix sediment very efficiently and the flow rates on these outlet rivers are high (rounded cobbles were in the river bed and appeared transported by it).*

This comment is similar to the specific comment 4 that we have already answered to (Page 7 – lines 22-23). We also remind this issue page 20 – line 16.

8. *Pg. 8 section 2.3. Please add some text saying how the glacial mass balance (and climate inputs) are calculated and refer to your table.*

We have added a Table (S1) in the supplementary materials and we explain how different parameters values have been chosen to calibrate our model. Furthermore, a short text was also added to describe the computation of the glacier mass balance (Supplementary material – Table S1).

9. *Fig. 4c, d - I suggest labelling the x-axis with the age plotted (e.g. "AHe Age" for c). Also - for the caption, mention what uncertainty you used for making the PDFs since this influences the smoothness of the curves relative to panel B. Caption should also explicitly say the data come from glacial outwash, not moraine.*

We have changed the figure label accordingly. However, the data used for the building of bedrock age distributions are the in-situ central ages of the AHe and AFT systems, through the age-elevation profiles, from Ehlers et al. (2015) and Enkelmann and Ehlers (2015) respectively, and thus are not from the glacial outwash sample presented in Ehlers et al. (2015). We describe these bedrock SPDF Page 12 – section 3.1.

10. *Pg12 ln7. Please say under what conditions the equilibrium state was calculated, and how closely it matches the present-day thickness and length of the glacier.*

We explain our calibration approach for the synthetic Tiedemann glacier Page 8 – lines 15-18. We also refer the readers to Figure S3, which shows the comparison between the iSOSIA model and the results of the ITMIX experiments (Farinotti et al., 2016) that predicts the ice thickness of many glacier around the world, as the Tiedemann glacier.

11. *Fig. 5. Please provide a more descriptive caption of what model this is at the start of the caption. Also - what are you actually doing with the 'hillslope' vs. 'glacial' parts of the catchment (Fig. 5a). It's not clear from the text (or caption) if you are also feeding hill slope material into the SPDFs calculated.*

Changes in the caption of Fig. 5 have been made to make it clearer (Figure 5 and Page 12 – line 26). We also added a sentence in the main text: "Particles are sampled independently of their source origin (hillslope vs glacial, Fig. 5a)."

12. *Pg13, ln1-2. Reword sentence please.*

Done. (Page 15 – lines 6-7).

13. *Fig. 6 - caption needs a starting sentence saying in general what is plotted and what model it comes from. Also- again for panel c, d - indicate the age type ("AHe Age") on the x-axis. Please do this for all other figures if this is also the case. It makes it much easier to read the figures quickly.*

Additional sentence and axes labels have been modified according to the comment for all figures.

14. *Pg.14 ln1. Please explain better what you mean by "model with uniform erosion". I'm confused because I don't understand how you made the ice model have uniform erosion - and where the uniform erosion was applied (e.g. Hillslopes and glacial areas?). Fig. 7e kinda gets at this, but the text should explain it better. Thanks.*

We forced uniform erosion by setting the production of particles in each model cell with a constant erosion rate. The erosion is applied in the entire model. The different colours in Figure 7a (i.e. red and blue) identify the sediment sources (hillslopes and glaciers). According to this comment and the following one, section 3.3. was confusing. We have therefore entirely rewritten it to make our results clearer. The model with uniform erosion is now explained more specifically at page 15 – lines 16-17.

15. *Pg. 16 top. After reading this page (related to previous comment) I'm still confused and some clarification is needed on this paragraph and what was actually calculated. The start of the*

*paragraph needs to explain better what the objective of this comparison is (hillslope vs. glaciers). Also ln3-4 are confusing because I thought this section only about uniform erosion, but this sentence says you are comparing a detrital SPDF to the uniform erosion model. Are you talking about the OBSERVED detrital SPDF? Perhaps make it clear throughout the text by always using 'observed' vs. 'modeled' detrital SPDFs*

As mentioned in a previous comment we have rewritten Section 3.3. We compared the modelled detrital SPDF with the modelled catchment bedrock SPDF resulting from the uniform erosion model. We differentiate between the detrital SPDF and the catchment bedrock SPDF clearer.

*16. Pg16, ln10+. This paragraph is also unclear. After reading all of section 3.3 - I'm confused as a reader. Please rewrite this section to make it clearer of a) what is the logic behind the experiment / comparison conducted, b) what is the first and second order main trends in the results and what data / model results (bedrock vs. Detrital you're looking at, and c) summary sentence(s) with the key observation to take away.*

We took into consideration this comment and have rewritten section 3.3. The rationale behind the model of uniform erosion was to characterise the form of the detrital SPDF at the glacier front resulting from a continuous spatially uniform production of particles (which differs from the model presented in Figure 5 that consider only a pulse of particle production). In this case, we should expect some effect due to the transfer time of sediment particles as we can see with the shifting of the mean detrital SPDF toward younger ages (Fig. 7). We discussed this effect in section 4.2.

*17. Maybe I missed it earlier, but after reading the results section - I think the methods section needs to be expanded some to explain how you look at (or calculate) hillslope vs. Glacial contributions to the detrital cooling ages.*

The particles can be sampled according to their source origin (each particle as a tag according to the source when forming that can be retrieved during the sampling process). We now specify this at the end of section 2.4 (Page12 – line 4).

*18. Pg16 ln 29. I don't understand how "we computed a new: : :". How did you compute this? Assuming uniform erosion? Using a diffusion based hill slope transport law? Please elaborate.*

We calculated a new bedrock SPDF using the age-elevation relationship convoluted to the hypsometric distribution of the hillslope sources, as we assume uniform erosion. We now refer to this bedrock SPDF as the "hillslope bedrock SPDF" in the main text. (Page 16 – lines 10-11)

*19. Pg.17 ln5-10. This result is entirely dependent on the assume hill slope transport law used, and diffusivity, : : :right? Perhaps mention this, and also make it clearer (per my previous comments) how the curve in Fig. 7 is calculated.*

Figure 7 displays results obtained with a uniform erosion model. There is therefore no dependency on the erosion law used for the hillslopes. Concerning a potential sensitivity to a transport law, because we consider steady-state SPDFs, our results are assumed independent of the transport processes or rate. We make this clearer by performing sensitivity tests by varying the diffusivity value used in this study ( $K_h = 5 \text{ m}^2 \text{ yr}^{-1}$ ). The results of these tests are presented in the supplementary materials. The mean detrital SPDFs (in the frontal moraine) resulting from particles originating from hillslopes are computed following the method presented in section 2.4. The hillslope bedrock SPDF is computed using the age-elevation relationship and the hypsometric distribution of the hillslope sources.

*20. Pg. 18 ln1. Several times in the paper you refer to or tune the model to an erosion rate 1 mm/yr. Why did you use this value? This should be explained in the methods section.*

We have used a value of 1 mm yr<sup>-1</sup> as it is in the range of natural values and it allows a continuous production of particles while maintaining a reasonable simulation time. We have added these sentences at the top of section 3.3 (Page 15 – lines 17-18).

21. Pg. 18 ln 1-4. *I don't understand this sentence and where these numbers you cite are coming from. For example, where is 31 mm/yr coming from? Where are the uncertainties in the numbers later in the sentence coming from?*

We meant that despite the mean erosion rate is 1 mm yr<sup>-1</sup>, local deviations to this average value occur due to the heterogeneous pattern of erosion. The value of 31 mm yr<sup>-1</sup> is the maximum local erosion rate shown in Fig. 9 (in the revised version of the manuscript). Next, we calculated the standard deviation for each sediment sources (hillslope vs glacial) to the average erosion rate of 1 mm yr<sup>-1</sup>. We clarify this in the revised version of the manuscript. (Page 18 – lines 17-19).

22. Pg. 18. Ln 6. *Please rewrite this sentence. I don't understand it.*

The sentence has been rephrased and split into 3 sentences (Page 18 – lines 19-21)

23. Pg. 19 ln 1. *“trading”? Not sure what you're trying to say.*

This sentence has been changed to clarify this.

23. Pg 19 ln 20. *Please expand this thought (particle tracking is in ice, not sub-glacial drainage). I would describe in general (qualitative) terms how the results could differ if subglacial outwash was sampled (e.g. how Ehlers et al. 2015 sampled).*

We have done so, see page 20 -lines 16-21.

24. Pg. 19. Ln 24-25 *“spatial erosion pattern can be biased on the detrital SPDF (e.g. Ehlers et al. 2015)”. Please remove the “e.g. Ehlers et al. 2015”. You may be correct that there is a bias, but you haven't shown this because the Ehlers et al. samples were from OUTWASH, not from ice. Also - your timescale arguments for bias later in the paragraph would likely be severely decreased if outwash is sampled because transit times of water to the outlet are significantly faster than for ice. So, please either show that Ehlers et al. 2015 have a bias in their outwash sample interpretation, or remove the reference to this paper to be fair. Final note concerning the general conclusions you are trying to make here about timescales - while your description is accurate for the simulations you present, it's hard to know if this is really a general result with any sensitivity tests to your model parameters presented in the study. Please consider adding sensitivity tests in the supplemental material and referring to them in the text. Table 1 - please be more specific about what you mean by “variable” in some rows. I think what you mean is that these variables are ‘internally calculated’*

The reference has been removed. The sensitivity tests have been added in supplementary materials, section 2. They show that the time to reach equilibrium, neglecting fluvial sediment transport, is of the same order than presented in the text (10<sup>3</sup> years), when varying the model parameters. Obviously, considering fluvial transport would decrease drastically the response time of sediment transport. Yet, because we are only considering the detrital signature of moraines, which are glacial sediment deposits and not fluvial ones, we do not expect a significant impact of considering fluvial transport on our results. We have revised the scope of our conclusion to account for this important point (Page 20 – lines 28-32 and Page 21 lines 1-11). Moreover, Table 1 has been modified according to the comment: “Variable” is replaced by “Model outcome”.

25. Pg. 21 ln 29-30. *This isn't really a surprise is it that moraines will more closely represent glacial erosion than hill slopes? Also - doesn't this statement and paragraph sort of contradict the previous section where you say there would be a bias towards low elevations in SPDFs? Maybe*

*I'm missing something here - but perhaps more text (in the previous section about biases) relating to what section 4.3 is saying would help clarify things more.*

In the case of debris-cover glaciers where the major sediment sources are hillslopes, thus moraines likely represent hillslopes erosion. We want to point out here that because glacial sediment particles are likely to be produced close to the ice streamline showing high velocities, the transfer time of such particles will be small compared to supraglacial sediment particle. Thus, in the case where the amount of erosion is the same for supraglacial and subglacial sources, we expect that the glacial sources to be over-represented, and thus the detrital SPDF to be bias toward younger ages if they are located beneath the ice (Page 23 – lines 13-16).

26. *Pg.22 section 4.4. This is nice that you done this analysis. However, to do this type of comparison you need to test if the distributions show in Fig. 10c are in fact statistically different. To do this, you need to apply a KS (or Kuiper) test of the distributions. Please include this type of analysis to see if these distributions really are in fact different at the 95% confidence level. This comment also potentially impacts the interpretations presented in section 4.5.*

We already reply in the general comment G4.

27. *Pg. 24 ln 1-2. This conclusion is correct for the simulations presented, but how variable is this result if there are variations in some of the model parameters. A sensitivity test of model inputs would help readers see if this result is general, or specific to your model simulations.*

We have made such tests and discussed the results in section 2 of the supplementary materials. The results do not significantly differ from those presented in the main text.

28. *Pg. 24 ln22-23 “However, we also emphasis : : :” This statement should be removed or significantly expanded & justified. How many grains should be sampled is a significant topic on it's own, and this study doesn't address this. The typical “100” grains minimum that people site from Vermeesch is not actually correct for these types of detrital samples (we have a paper in preparation that goes through the statistics of number of detrital AHe samples needed for different catchment sizes and it's complicated).*

We removed this sentence from the conclusion.

29. *Supplementary materials. There is useful material presented in the supplement, but the figure captions are a too sparse for some figures. Please expand the figure captions some to be more descriptive of what is shown. For example, what model simulation is shown in the figure, and perhaps also what section of the text the figure is relevant to.*

The captions of the figures have been rewritten, expanded and clarified for better description of the figures.

## **Reference**

Vermeesch, P.: Dissimilarity measures in detrital geochronology. *Earth-Science Reviews*, 178, 310-321, 2018.

# ***Interactive comment on “Modelling the effects of ice transport and sediment sources on the form of detrital thermochronological age probability distributions from glacial settings” by Maxime Bernard et al.***

**Response to the reviewer.**

**We thank the anonymous reviewer for his review of the manuscript. We here response to the main concern of the anonymous reviewer and then we provide a point by point response to his comments.**

We first point out that we changed the title of the manuscript to be more informative about the approach of our study.

The first concern is about the limited sediment transport processes considered in our study. We considered the transport of sediments on hillslopes and by ice but do not incorporate transport by meltwater. The anonymous reviewer pointed out that the majority of sediments is transported out of the glacier through the subglacial hydrology system. This may have important implications concerning the sediment transfer time and thus on the equilibrium time of the frontal moraine reported in our study (about 1500 years). We understand and share the concern of the anonymous reviewer about the role of subglacial hydrological systems in reducing the transfer time of sediments. We have revised the scope of our conclusions to discuss this important point. However, as we only consider the detrital signature of moraines, which are glacial sediment deposits and not fluvial ones, we do not expect a significant impact of fluvial transport on our results. We also discuss this point further in the revised version of the manuscript in section 4.2.

Our time for equilibrium of the frontal moraine (i.e. 1500 years) is similar to the characteristic time estimated by some authors the anonymous reviewer has cited. However, as mentioned earlier, we expect that the frontal moraine mainly reflects the glacier dynamics as the sediments that participate to build such glacial features mainly come from the ice (e.g. Winkler and Matthews, 2010; Bowman et al., 2018; Ewertowski and Tomczyk, 2020). Moreover, our discussion includes a spatial distribution on sediment transfer times which is not captured by the equation estimating the characteristic time. For these reasons we limited our discussion to sediment transfer times but revised the scope of our conclusion.

Initially, we did not aim to compare our results explicitly to the observations given that our synthetic steady Tiedemann glacier dynamics does not reflect the real Tiedemann glacier which is currently retreating. However, the comments of the two reviewers convinced us to consider such comparison. We now compare our modelled detrital AFT distributions to the detrital AFT distributions from Enkelmann and Ehlers (2015) which are coming from ice-cored terminal moraine (see Section 4.4).

We are aware that the erosion rule of Ugelvig et al. (2016) is mainly based on a mechanical model for bedrock fractures (Iverson, 2012), which has not been validated by a comparison with field data. On the other hand, empirical models that consider power laws between erosion rates and sliding velocity obtained by fitting natural data have little physical support and may lack some important processes. For instance, it is well documented that effective pressure plays a role in the quarrying process (e.g. Cohen et al., 2006). The equation of Ugelvig et al. (2016) is an attempt to incorporate this effect on a large-scale model. As discussed in Ugelvig et al. (2016), the strong dependency of erosion to the effective pressure (the power of 3) may be exaggerated. However, the results presented in Fig. 9, do not contradict the observations. If we consider the mean catchment erosion rate ( $1 \text{ mm yr}^{-1}$ ) and the maximum sliding speed of the main glacier ( $\sim 60 \text{ m yr}^{-1}$ , Fig. 3), we are in the range of values

presented in Cook et al. (2020). Overall, we chose this model because of its mechanistic basis, despite its lack of a validation by natural data.

We share the concern of the anonymous reviewer about the availability of the source code. Therefore, we now make the code for iSOSIA and the external routine for constructing age distributions publicly available. (<https://github.com/davidlundbek/iSOSIA>).

### **Specific comments:**

1. *Abstract: How does detrital thermochronology enables to avoid biases better than other methods?*

We did not make a comparison to other methods, but meant that thermochronological analysis on sediments (detrital thermochronology) potentially provides information from beneath the glacier, contrary to in-situ thermochronology for which sampling beneath the ice is generally not possible. (Page 1 – line 10).

2. *Page 1-line 22: SPDF should be spelled out the first time it is used.*

Done.

3. *Page 2 – line 3: The authors should be more precise on the order of timescales.*

This point has been removed from the abstract.

4. *Page3 – lines 5-17: Detrital studies can only be done appropriately, in my opinion, if the source area is properly described. The fertility or age distribution within the catchment must be characterized as much as possible. It is clearly not the panacea as the problem remains ill-posed, but at the very least the authors could make some references about the importance of having a good knowledge of the source area.*

We share the concern of the anonymous reviewer. Therefore, we have added a small paragraph in the introduction to mention the need of a priori knowledges on the spatial distribution of ages in the catchment and mineral fertility, to interpret the detrital thermochronology data (Page 3 – line 10-11).

5. *Page 4 – lines 9-10: The code should be made publicly available.*

The iSOSIA version to run models presented in this study, and the Matlab code to compute age distributions, is now publicly available.

6. *Page 6 – line 11: “We follow MacGregor et al. (2009)..” and everybody else (e.g. Braun et al., 1999; MacGregor et al. 2000; Tomkin and Braun, 2002, etc.)*

We are aware that other authors considered the same assumption about ignoring the abrasion erosion, however to limit the number of references used in this study we now limit our citation to MacGregor et al. (2009).

7. *Page 6 – line 19: While there are some observations that support the link between sliding and erosion (e.g. Humphrey and Raymond, 1994; Herman et al., 2015; Koppes et al., 2015; Cook et al., 2020), there is no available data specifically for the chosen erosion rule, beyond the models of Ugelvig et al. (2018). It would be good at least if the authors could acknowledge some of the observational basis for utilizing of this rule, or the relationship between sliding and erosion.*

We already answered this comment in the responses to the main comments.

8. *Page 6 – line 22: I do not think subglacial fluvial transport should be ignored.*

Indeed, we fully agree that subglacial fluvial transport should be considered in future studies. However, the role of subglacial fluvial transport in the building of frontal moraines may be not predominant. We discuss this point further in the section 4.2 of the new version of this study.

9. *Page 7 – line 22: The flux and erosion rate (i.e., velocity) are the same equations (Eqns. 7 and 8) both scale with constant that have the same unit. That cannot be.*

We thank the reviewer to have pointed out this mistake. This has been corrected in the new version of the manuscript.

10. *Page 7 – line 10: The authors assume that all the transport happens within the ice.*

We have answered this comment in the responses of the general comments.

11. *Page 8: Is there any information on the actual velocity of the glacier? The authors have chosen a relatively slow glacier, although the glacier is comparable to many alpine glaciers and I appreciate that the authors need a site where some thermochronological data were available. This has some influence on the final result of the characteristic timescale, as it scales as the ratio between the glacier length and velocity. For example, Cook et al. (2020) showed velocities ranging from a few meters per year to several kilometres, implying that the equilibrium timescale estimated here is only applicable to the Tiedeman glacier.*

To our knowledge, the only information on the velocity of the glacier comes from the ITMIX experiments (Farinotti et al., 2016, 2019). We share the concern of the reviewer about the characteristic timescale; however, we stress that showing the spatial distribution of sediment transfer times brings additional information relative to a single characteristic timescale, that may hide large variability. We also agree that the variability from glacier to glacier (Cook et al., 2020) may restrict the generality of the conclusion about the equilibrium timescale to the Tiedemann glacier, but we think of this conclusion more as an insight about the equilibrium timescale of the frontal moraine, and its relevance to the interpretation of detrital SPDFs. Future studies should explore this issue.

12. *Page 10 – line 11: It would be useful to have more information about the geology. Ehlers et al. (2015) refer to Rusmore and Woodsworth, but the geological map is very large. Is the geology under the glacier truly uniform? I could not find this information.*

The more recent and precise geological map of the Tiedemann glacier area is from Cui et al. (2017) and is available [here](#). The main lithologies outcropping in the Tiedemann glacier catchments are granodiorite and orthogneiss as mentioned in Ehlers et al. (2015), and suggest low bias in fertility of apatite in the area.

13. *Page 12 - line 4: 'limiting the ability' I do not understand why. Intuitively, more variations, such as kink in an age-elevation profile should provide more information.*

A kink in an age-elevation profile give more information in terms of exhumation history. However, the ability to track the source of sediments depends on the uniqueness of the age-elevation relationship (i.e. one age = one elevation). For the AFT age-elevation profile, this is not the case as the same age can be interpreted as two very different elevation.

14. *Page 12 - lines 14-16: The time to travel through the glacier is entirely dependent on the ice flow model, and it is likely it would be significantly faster if the subglacial hydrology would be included.*

We agree that transport by meltwaters would decrease the transfer time of sediments to the glacier margin and should be integrated in future studies. However, we postulate that the debris composing frontal moraine are mainly the reflect of the ice dynamics, as their formation is mainly done through dumping of sediment from the ice surface, and bulldozing process (see section 4.2).

15. Page 19 – line 15: *There are numerous papers on the glacier response time that could be cited.*

We included references on the glacier response time in the new version of the manuscript, including Jóhannesson et al. (1989); Oerlemans (2001) Roe and O’Neal (2009); Herman et al. (2018).

### References:

Benn, D., and Evans, D. J.: *Glaciers and glaciation*. Routledge, second edition, New York, USA, 2013.

Bowman, D., Eyles, C. H., Narro-Pérez, R., & Vargas, R.: Sedimentology and Structure of the Lake Palcacocha Laterofrontal Moraine Complex in the Cordillera Blanca, Peru. *Revista de Glaciares y Ecosistemas de Montaña*, (5), 16-16, 2018.

Cook, S. J., Swift, D. A., Kirkbride, M. P., Knight, P. G., and Waller, R. I.: The empirical basis for modelling glacial erosion rates. *Nature communications*, 11(1), 1-7, 2020.

Cui, Y., Miller, D., Schiarizza, P., and Diakow, L.J.: British Columbia digital geology. British Columbia Ministry of Energy, Mines and Petroleum Resources, British Columbia Geological Survey Open File 2017-8, 9p. Data version 2019-12-19, 2017.

Ewertowski, M. W., and Tomczyk, A. M., Reactivation of temporarily stabilized ice-cored moraines in front of polythermal glaciers: Gravitational mass movements as the most important geomorphological agents for the redistribution of sediments (a case study from Ebbabreen and Ragnarbreen, Svalbard). *Geomorphology*, 350, 106952, 2020.

Farinotti, D., Brinkerhoff, D., Clarke, G. K., Fürst, J. J., Frey, H., Gantayat, P., ... and Linsbauer, A.: How accurate are estimates of glacier ice thickness? Results from ITMIX, the Ice Thickness Models Intercomparison eXperiment. *The Cryosphere Discussions*, 2016.

Farinotti, D., Huss, M., Fürst, J. J., Landmann, J., Machguth, H., Maussion, F., and Pandit, A.: A consensus estimates for the ice thickness distribution of all glaciers on Earth. *Nature Geoscience*, 12(3), 168, 2019.

Herman, F., Braun, J., Deal, E., and Prasicek, G.: The response time of glacial erosion. *Journal of Geophysical Research: Earth Surface*, 123(4), 801-817, 2018.

Jóhannesson, T., Raymond, C. F., and Waddington, E. D.: A simple method for determining the response time of glaciers. In *Glacier fluctuations and climatic change* (pp. 343-352). Springer, Dordrecht, 1989.

Oerlemans, J.: *Glaciers and climate change*. CRC Press, 2001.

Roe, G. H., and O’Neal, M. A.: The response of glaciers to intrinsic climate variability: observations and models of late-Holocene variations in the Pacific Northwest. *Journal of Glaciology*, 55(193), 839-854, 2009.

Ugelvig, S. V., Egholm, D. L., and Iverson, N. R.: Glacial landscape evolution by subglacial quarrying: A multiscale computational approach. *Journal of Geophysical Research: Earth Surface*, 121(11), 2042-2068, 2016.

Winkler, S., and Matthews, J. A.: Observations on terminal moraine-ridge formation during recent advances of southern Norwegian glaciers. *Geomorphology*, 116(1-2), 87-106, 2010.

# **The Modelling the effects of ice and hillslope erosion and detrital transport and sediment sources on the form of detrital thermochronological age probability distributions from glacial settings**

5 Maxime. Bernard<sup>1</sup>, Philippe. Steer<sup>1</sup>, Kerry. Gallagher<sup>1</sup>, David Lundbek. Egholm<sup>2</sup>

<sup>1</sup>Univ Rennes, CNRS, Géosciences Rennes, UMR 6118, 35000 Rennes, France.

<sup>2</sup>Department of Geoscience, Aarhus University, Aarhus, Denmark.

**Correspondence:** Maxime Bernard (maxime.bernard@univ-rennes1.fr)

**Abstract.** The impact of glaciers on the Quaternary evolution of mountainous landscapes remains controversial. Although in situ or bedrock low-temperature thermochronology offers insights on past rock exhumation and landscape erosion, the ~~methods~~ method also ~~suffers~~ suffers from potential biases due to the difficulty of sampling bedrock buried under glaciers. Detrital thermochronology attempts to bypass ~~overcome~~ this issue by sampling sediments, at e.g. the catchment outlet, ~~that a component of which~~ may originate from beneath the ice. However, ~~the detrital~~ age distributions ~~resulting from detrital thermochronology do~~ not only reflect the catchment exhumation, but also the spatially variable patterns and rates of surface erosion and sediment transport. In this study, we use a new version of a glacial landscape evolution model, iSOSIA, to address the effect of erosion and sediment transport by ice on the form of synthetic detrital age distributions. Sediments are tracked as Lagrangian particles ~~which can be~~ formed by bedrock erosion, ~~transported by and their transport is restricted to~~ ice or hillslope processes and until they are deposited. We apply ~~base~~ our model ~~to~~ on the Tiedemann glacier (British Columbia, Canada), which has simple morphological characteristics, such as a linear form and no connectivity with large tributary glaciers. Synthetic detrital age distributions are generated by specifying an erosion history, then sampling sediment particles at the frontal moraine of the modelled glacier.

~~An assessment of sediment transport shows that 1500 years are required to reach an equilibrium for detrital particle age distributions, due to the large range of particle transport times from their sources to the frontal moraine. Next, varying sampling locations and strategies at the glacier front leads to varying detrital SPDFs, even at equilibrium. These discrepancies are related~~ Results show that sediment sources, reflecting different processes such as glacier and hillslope erosion, can have distinct bedrock age distribution signatures, and estimating such distributions should help to identify predominant sources in the sampling site. However, discrepancies between the detrital and the bedrock age distributions occur due to (i) the selective storage of a large proportion of sediments in small tributary glaciers and in lateral moraines, (ii) the large range of particle transport times, due to varying transport lengths and to a strong variability of glacier ice velocity, (iii) the heterogeneous pattern of erosion, (iv) the advective nature of glacier sediment transport, along ice streamlines, ~~that~~. This last factor leads to a poor

lateral mixing of particle detrital signatures inside the frontal moraine: and then local sampling of the frontal moraine is likely to reflect local sources upstream. Therefore, sampling randomly across the moraine is preferred for a more representative view of the catchment age distribution. Finally, systematic comparisons between synthetic (U-Th)/He and fission track detrital ages, with different bedrock age-elevation profiles and different relative age uncertainties, show that ~~(i)~~ the nature of the age-elevation relationship and age uncertainties largely ~~controls/control~~ the ability to track sediment sources, ~~and (ii) in the detrital record.~~ However, depending on the erosion pattern spatially, qualitative first-order information may still be extracted from thermochronological system with high uncertainties ( $> 30\%$  ~~depending on erosion pattern.~~). Overall, our results demonstrate that detrital age distributions in glaciated catchments are strongly impacted not only by erosion and exhumation but also by sediment transport processes and their spatial variability. ~~Combined~~ However, when combined with bedrock age distributions, detrital thermochronology offers a novel means to constrain the transport pattern and time of sediment particles. ~~However, our results also suggest that detrital age distributions of glacial features like frontal moraines, are likely to reflect a transient case as the time required to reach detrital thermochronological equilibrium is of the order of the short timescale glacier dynamics variability, as little ice ages or recent glaciers recessions.~~

## 1 Introduction

Glaciers have left a profound impact on the topography of mountainous landscapes in particular by eroding deep glacial valleys and depositing large volume of sediments in moraines. As glacier dynamics are linked to climate, an active area of research aims to characterize the role of glacial erosion on the dynamics and relief development of mountain belts during the recent Quaternary glaciations (e.g. Zachos et al., 2001; Molnar and England, 1990; Beaumont et al., 1992; Montgomery, 2002; Brozović et al., 1997; Whipple et al., 2009; Steer et al., 2012; Champagnac et al., 2014). To address these questions, two timescales have typically been considered: a longer timescale ( $10^5$ - $10^6$  years) to assess the potential glacial imprint on the landscape, and a shorter timescale ( $10^1$ - $10^4$  years) to understand how ice actually erodes the landscape. For example, some studies integrated glacial sediment records worldwide and in situ low-temperature thermochronology data, to estimate glacial erosion rates. They showed average erosion rates of  $10^0$ - $10^3$  mm yr<sup>-1</sup> on short timescales ( $10^3$ - $10^5$  years) and long-term ( $>10^6$  years) average erosion rates of  $10^{-2}$ - $10^0$  mm yr<sup>-1</sup> (Hallet et al., 1996; Koppes and Montgomery, 2009; Valla et al., 2011b; Koppes et al., 2015; Bernard et al., 2016).

Herman et al. (2013) used a global compilation of in situ thermochronological data and an inverse approach to infer an increase in erosion rates for all mountain ranges in the Quaternary period. They suggested that this effect is more pronounced for glaciated mountains, ~~suggesting~~ implying a significant role of glaciation on erosion rates. However, the results of this study have been contested (Willenbring et al., 2016; Schildgen et al., 2018) and ~~the link between the long-term glaciation and an increase of erosion rates is still debated,~~ thus the conclusion debated. More recently, Yanites and Ehlers (2016) correlated high glacier ice sliding velocities with high denudation rates deduced by thermochronological data in the southern Coast Mountains, British Columbia. They also found that glacial erosion may only occurs for less than 20% of a glacial-interglacial cycle, in

~~some areas, and may explain the discrepancy between the longer and shorter timescale for erosion rates.~~ In situ thermochronology consists of collecting bedrock samples from discrete locations to map thermochronological ages and exhumation rates (e.g., Fitzgerald and Stump, 1997; Valla et al., 2011b, Herman et al., 2013). However, this approach offers a potentially biased assessment of catchment wide exhumation pattern as it is dependent on the spatial bedrock sampling strategy (Ehlers, 2005, Valla et al., 2011a). For example, the age-elevation relationship inferred from in situ ~~or bedrock~~ thermochronology ~~data~~ may not ~~account for young thermochronological capture younger~~ ages expected along the valley floor, and buried under the ice (Enkelmann et al., 2009; Grabowski et al., 2013).

In glacial ~~environment~~~~environments~~, erosion mostly occurs subglacially through abrasion and quarrying (Boulton, 1982; Hallet et al., 1996) or supraglacially (i.e. ice-free areas) through periglacial mechanisms and gravitational processes (Matsuoka and Murton, 2008). These two sources (i.e. supraglacial and subglacial areas), and their contribution to erosion, define the relative proportion of sediments that enter the glacier transport system (Small, 1987). Sediments are transported by glaciers by (i) subglacial water flow through cavity or channel systems (Kirkbride, 2002; Alley et al., 1997; Spedding, 2000), and (ii) by ice internal deformation for sediments incorporated within or above the ice (Hambrey et al., 1999; Goodsell et al., 2005).

Therefore, sampling and analysing these sediments ~~(with detrital thermochronology)~~ has the potential to provide a more spatially integrated view of the catchment erosion pattern on short timescales ( $10^1$ - $10^4$  years) and thereby a more representative indication of how ice is eroding the landscape (e.g. Stock et al., 2006; Tranel et. 2011; Ehlers et al., 2015). The detrital sampling protocol focusses on collecting glacial deposits, generally close to the outlet of the catchment (Ruhl and Hodges, 2005; Stock et al., 2006; Falkowski et al., 2016; Glotzbach et al., 2018). A major motivation for detrital sampling is that we can potentially obtain grains from regions inaccessible for bedrock sampling due to ice cover and lack of outcrop or, more pragmatically, logistical considerations (e.g. cost). ~~However, a priori knowledges about the distribution of thermochronological ages with elevation (e.g. Brewer et al., 2003), and the mineral fertility of the sources (Moecher and Samson, 2006), are often required to reliably interpret the data from detrital thermochronology.~~

Thermochronological age distributions of detrital samples are generally ~~interpreted in terms of~~~~presented as~~ synoptic probability density functions (SPDF) (Brewer et al., 2003; Ruhl and Hodges., 2005). Analysis of many ~~glacial~~~~glaciated~~ catchments has been based on the interpretation of these SPDFs (Stock et al., 2006; Tranel et al., 2011; Avdeev et al., 2011; Thomson et al., 2013). More recently, Enkelmann and Ehlers (2015) ~~and Ehlers et al. (2015)~~ investigated the ~~erosion patterns and the~~ degree of mixing of ~~ice-cored~~ sediments ~~from ice cores~~ at the terminus of the Tiedemann glacier (Coast Mountains, Canada) using both detrital and in situ low-temperature thermochronology. ~~By comparing~~ ~~Comparison of~~ the ~~bedrock and~~ detrital age distributions, ~~they inferred from the ice-cored terminal moraine and from glacial outwash (Ehlers et al., 2015), showed~~ that sampling through the terminal moraine is similar to sampling the ~~pre-glacial rivers~~~~proglacial river~~, supporting the idea of an efficient ~~vertical~~ mixing of glaciated sediments at the ~~glaciers~~~~glacier~~ front. The latter result is also consistent with results obtained on the Malaspina Glacier, Alaska (Enkelmann et al., 2009; Grabowski et al., 2013). However, ~~the authors~~~~Enkelmann and Ehlers (2015)~~ pointed out the sensitivity of their results to the relatively high ~~age~~ uncertainties ~~of on the data~~~~ages~~. Furthermore, while the shape of ~~detrital~~ SPDFs is expected to be mainly controlled by the catchment exhumation history, other

processes such as grain erosion, transport and deposition are likely to also influence the form of SPDFs. These factors will contribute to the overall integration of the spatially variable products of erosion into the sediment ultimately deposited at the outlet play a role. Consequently, characterizing the effect of surface processes on the shape of detrital SPDFs may help improve their interpretation.

- 5 In this study, we address the present a numerical approach that allows us to explore the effect of sediment transport by the ice and the role of the different source areas (i.e. subglacial and supraglacial) in the shaping of detrital SPDFs at a glacier front. To this end, we combined a new version of a glacial landscape evolution model, iSOSIA (Egholm et al., 2011) that allows tracking of sediments, with an external routine that calculates the detrital thermochronological ages. To this end, we use age distributions. We chose to apply our numerical models simulating approach on the Tiedemann glacier catchment, as it
- 10 shows simple morphological characteristics and because thermochronological data are available (Enkelmann and Ehlers, 2015; Ehlers et al., 2015). We produced our bedrock synthetic thermochronological data from two low-temperature thermochronological systems, apatite (U-Th)/He and apatite fission track (i.e. AHe and AFT respectively), according to the age-elevation profiles from Enkelmann and Ehlers (2015) for the AFT ages and from Ehlers et al. (2015) for the effect of surface processes, including erosion and AHe ages. First, we investigate the kinematics of our sediment transport by the ice, on the detrital SPDFs that we compare with model in the modelled catchment, to assess the bedrock age distribution. We take advantage of a new version of role of the glacial landscape evolution model iSOSIA (for integrated Second Order Shallow Ice Approximation, Egholm et al., 2011) that includes sediment particle tracking. First, we ice transport. Next, we focus on the description role of the dynamics of sediment transport within the modelled catchment. Second, we perform three numerical simulations that consider (i) sources by calculating detrital SPDFs resulting from uniform catchment erosion, (ii) glacial-only erosion, and (iii) across the catchment, as well as, hillslope-only erosion. These experiments allow us to explore the influence of 1) ice transport and 2) sediment source areas, both subglacial and supraglacial, on the shape of the detrital SPDFs, sources and glacial-only eroded sources. Finally, we consider non-uniform catchment erosion, by letting iSOSIA and its implicit erosion laws control the pattern of erosion. This last experiment allows us to assess the record of such complex erosion processes potentially contained in the shape of detrital SPDFs. For each experiment, we produce synthetic all experiments, the
- 25 sediments are transported by ice and hillslopes, so that transport by the hydrological system is neglected. The two thermochronological data for two routinely used low-temperature thermochronological systems, apatite (U-Th)/He and apatite fission track methods (i.e. AHe and AFT respectively). These two methods and AHe considered, have different thermal sensitivities and so thus, different spatial distributions of bedrock ages in the pre-glacial landscape. They also typically have different age uncertainties allowing us to address the effect of these uncertainties on the interpretation of
- 30 SPDFs.

## 2 Methods

### 2.1 The glacial landscape evolution model: iSOSIA

iSOSIA is a one-layer depth-integrated second order shallow ice approximation model (Egholm et al., 2011). It is able to simulate ice flowing on relatively steep topography, through the computation of membrane stresses (Hindmarsh, 2006) and with a depth-integrated ice flow velocity. These two characteristics make iSOSIA more accurate than models based on the zeroth-order shallow ice approximation, while being ~~computational~~computationally efficient compared to models that resolve the full 3D set of Navier-Stokes equations (Elmer/Ice, Braedstrup et al., 2016). A full description of iSOSIA and the relevant ice flow equations can be found in Egholm et al. (2011, 2012a, 2012b) and Braedstrup et al. (2016).

Glacial hydrology plays an important role on the ice sliding velocity (Clarke, 1987), and has been recently investigated in numerical models (Schoof, 2005, 2010; Iverson, 2012; Ugelvig et al. 2016; Ugelvig et al. 2018). Here we adopt a simplified version of the sliding law of Schoof (2005), that accounts for the opening of cavities due to the roughness of the bed. This defines the area on which the basal shear stress ( $\tau_b$ ) is applied as well as the basal sliding speed ( $u_b$ ), as below

$$u_b = C_s \cdot \frac{\tau_b^n}{C}, \quad (1)$$

where  $C_s$  is the ice sliding constant and  $C = 1 - \frac{S}{L}$  defines the proportion area on which  $\tau_b$  is applied, where  $L$  is the length between two topographic steps (Fig. S1). The steady-state length of cavities ( $S$ ) is controlled by the effective mass balance (i.e. accounting for basal and internal melting of the ice) that determines the annual average water flux over the glacier,  $q_w$ . This is specified as follows

$$S = \left( \frac{L_s \cdot q_w}{k_0 \cdot \sqrt{\nabla\psi}} \right)^{0.8} \cdot \frac{1}{\beta \cdot h_s}, \quad (2)$$

where  $L_s$  is the mean cavity spacing in a cell (see Table 1 for all parameter values),  $k_0$  is the minimum hydraulic conductivity,  $\nabla\psi = \rho_w g \nabla h_{ice}$  the hydrological head,  $\beta$  is a scaling factor, and  $h_s$  is the mean height of the topographic step and depends

**Table 1:** List of parameters described in the text.

linearly on the slope in direction of sliding (see Ugelvig et al., 2016; Eq. 10). The term in parentheses on the right hand side of Eq. (2) represents the cross-sectional area of a cavity ( $A_c$ ). The steady cavity size controls the effective pressure ( $N$ ) of the system and influences the basal sliding speed. However, due to how cavities dictate the volume of water stored at the bed, the effective pressure is also influenced by the opening/closure rate of cavities following

$$N = B \left( \frac{g}{\pi} \right)^{\frac{1}{n}} \left[ \frac{u_b h_s - \beta h_s \frac{\partial S}{\partial t}}{S^2} \right]^{\frac{1}{n}}, \quad (3)$$

Parameters	Description	Value/Unity
Climate		

Mis en forme : Position :Horizontal : Gauche, Par rapport à : Colonne, Vertical : En ligne, Par rapport à : Marge, Horizontal : 0 cm, Renvoi ligne automatique

Mis en forme : Position :Horizontal : Gauche, Par rapport à : Colonne, Vertical : En ligne, Par rapport à : Marge, Horizontal : 0 cm, Renvoi ligne automatique

Tableau mis en forme

$T_{sl}$	Sea level temperature	$9^{\circ} \text{C}$
$dT_{air}$	Lapse rate	$0.006^{\circ} \text{C m}^{-1}$
$m_{acc}$	Accumulation gradient	$0.08 \text{ m.yr}^{-1} \text{ }^{\circ} \text{C}^{-1}$
$m_{abl}$	Ablation gradient	$0.25 \text{ m.yr}^{-1} \text{ }^{\circ} \text{C}^{-1}$
<b>Ice</b>		
$n$	Ice creep constant	3.0
$B$	Ice viscosity constant	$73.3 \times 10^6 3 \times 10^6 \text{ Pa s}^{1/3}$
$C_s$	Ice sliding constant	$1.29 \times 10^{-2} \text{ Pa s}^{1/3}$
$h_{ice}$	Ice surface elevation	Variable Model outcome
$H$	Ice thickness	Variable Model outcome
$\nabla b_s$	Bed slope in direction of ice flow	Dimensionless
$k_q$	Quarrying coefficient for erosion	$1.97 \times 10^{-4} \text{ s Pa}^{-3}$
<b>Hillslope</b>		
$S_c$	Critical slope	1.4
$K_h$	Hillslope diffusivity	$5 \text{ m}^2 \text{ y}^{-1}$
$k_{eh}$	Hillslope erosion coefficient	$3.95 \times 10^{-5} \text{ m}^2 \text{ y}^{-1}$
<b>Particles</b>		
$H_s$	Particle sediment thickness	0.01 m
$Z_p$	Burial depth of particles relative to the ice surface	Dimensionless
<b>Hydrology</b>		
$N$	Effective pressure	Variable Model outcome
$h_s$	Bed step height	Variable Model outcome
$S$	Cavities size	Variable Model outcome
$L$	Bed step length	Variable Model outcome
$L_s$	Cavity spacing	4 m
$k_0$	Minimum hydraulic conductivity	$3.10 \times 10^{-4} \text{ kg}^{-1/2} \text{ m}^{3/2}$
$q_w$	Water flux	Variable
$\nabla \psi$	Hydrological gradient	$\nabla \psi = q_w g \nabla h_{ice}$
$\beta$	Cavity shape parameter	0.7

linearly on the slope in direction of sliding (see Ugelvig et al., 2016; Eq. 10). The term in parentheses on the right-hand side of Eq. (2) represents the cross-sectional area of a cavity ( $A_c$ ). The steady cavity size controls the effective pressure (N) of the system and influences the basal sliding speed. However, due to how cavities dictate the volume of water stored at the bed, the effective pressure is also influenced by the opening/closure rate of cavities following

Mis en forme : Position :Horizontal : Gauche, Par rapport à : Colonne, Vertical : En ligne, Par rapport à : Marge, Horizontal : 0 cm, Renvoi ligne automatique

Mis en forme : Position :Horizontal : Gauche, Par rapport à : Colonne, Vertical : En ligne, Par rapport à : Marge, Horizontal : 0 cm, Renvoi ligne automatique

Mis en forme : Position :Horizontal : Gauche, Par rapport à : Colonne, Vertical : En ligne, Par rapport à : Marge, Horizontal : 0 cm, Renvoi ligne automatique

Mis en forme : Position :Horizontal : Gauche, Par rapport à : Colonne, Vertical : En ligne, Par rapport à : Marge, Horizontal : 0 cm, Renvoi ligne automatique

Mis en forme : Position :Horizontal : Gauche, Par rapport à : Colonne, Vertical : En ligne, Par rapport à : Marge, Horizontal : 0 cm, Renvoi ligne automatique

Mis en forme : Position :Horizontal : Gauche, Par rapport à : Colonne, Vertical : En ligne, Par rapport à : Marge, Horizontal : 0 cm, Renvoi ligne automatique

Mis en forme : Position :Horizontal : Gauche, Par rapport à : Colonne, Vertical : En ligne, Par rapport à : Marge, Horizontal : 0 cm, Renvoi ligne automatique

Mis en forme

**Table 1:** List of parameters described in the text.

$$N = B \left( \frac{8}{\pi} \right)^{\frac{1}{n}} \left[ \frac{u_b h_s - \beta h_s \frac{\partial S}{\partial t}}{S^2} \right]^{\frac{1}{n}},$$

(3)

where  $B$  and  $n$  are the ice creep parameters. This hydrological model is similar to that used in Ugelvig et al. (2016), and we therefore refer the reader to this study for more details. We calibrated our hydrological model by a trial-error process by varying  $k_0$  (Eq.2) to produce a reasonable value of basal ice sliding velocities (Table S1).

In iSOSIA, the mass balance  $M$  is linearly proportional to the mean annual air temperature  $T_{air}$ :

$$M = \begin{cases} -m_{acc}T_{air}, & \text{if } T_{air} \leq 0 \\ -m_{abl}T_{air}, & \text{if } T_{air} > 0 \end{cases} \quad (4)$$

where  $m_{acc}$  and  $m_{abl}$  are the mass accumulation and the ablation gradients with respect to temperature, respectively.  $T_{air}$  is assumed to decrease linearly with elevation  $h$  with a lapse rate  $dT_{air}$  as

$$T_{air} = T_{sl} + dT_{air} \cdot h, \quad (5)$$

where  $T_{sl}$  is the sea level temperature set constant at 9°C.

As mentioned in the introduction, the two main mechanisms of glacial erosion are abrasion and quarrying (Boulton, 1982; Hallet et al., 1996). As debris resulting from abrasion is mostly small in size (i.e. <50  $\mu\text{m}$ , Hallet, 1979), we follow MacGregor et al. (2009) and consider that this debris is instantaneously transported away from the glacial catchment by meltwater/meltwaters. However, quarrying acting on the lee side of bedrock steps by plucking can produce larger debris. Therefore, we consider in this study that sediments are only produced by quarrying. Quarrying is generally accounted for by a classical power-law basal sliding power-law, modified to account for some factors directly related to plucking (MacGregor et al. 2000; Kessler et al., 2008; MacGregor et al., 2009; Egholm et al., 2009; Herman et al., 2011). These factors include pre-existing fractures in the bedrock, effective pressure, the regional bed slope in direction of ice flow, variation in meltwater drainage and the ice-bed contact area determined by the opening of cavities (Iverson, 2012; Cohen et al., 2006; Ugelvig et al., 2016; Anderson, 2014; Ugelvig et al., 2018). We follow Ugelvig et al. (2016) in modelling the quarrying rate  $E_q$  as

$$E_q = k_q N^3 u_b (\nabla b_s + b_{s0})^2, \quad (6)$$

where  $k_q$  is a scaling coefficient for the effective pressure,  $N$ , that represents the effect of bedrock lithology and fractures,  $\nabla b_s$  is the bed slope in direction of sliding and  $b_{s0}$  is a term to allow for negative bed slopes. As we focus on glacier-induced erosion, we ignore fluvial erosion and transport. However, we do consider hillslope erosion, which represents the supraglacial source of sediments. We assume that hillslope erosion,  $E_h$ , depends non-linearly on the bed gradient, as defined in (Andrew and Bucknam, 1987) and (Roering et al., 1999):

$$E_h = \frac{k_{eh} \nabla b}{1 - \left(\frac{|\nabla b_{ij}|}{S_c}\right)^2}, \quad (7)$$

$$E_h = - \frac{k_{eh} \cdot \nabla b}{1 - \left(\frac{|\nabla b_{ij}|}{S_c}\right)^2} \frac{dt}{dl}, \quad (7)$$

where  $k_{eh}$  is an erodibility constant, and  $S_c$  the critical slope. dt the time step and dl the resolution of a cell (dl = 100 m).

## 2.2 Particle tracking and sampling

To investigate calculate the detrital age distribution distributions produced from a glaciated catchment, we need to track sediments from the source to their final site of deposition. Accordingly, we define “particles” as sediment trackers in our models. Sediments are produced as a result of local erosion. When sediment thickness exceeds a threshold  $H_s = 0.01$  m, a particle is generated and can be transported away from its initial cell. This threshold is chosen to lead to a reasonable number of particles within models while keeping a sufficient time resolution in the generation of particles (i.e. with an erosion rate of  $1 \text{ mm yr}^{-1}$  and  $H_s = 0.01$  m a particle is generated every 10 years in a cell). Depending on its position within the catchment, a particle is transported by different processes. Similar to Eq. (7), we assume that the flux,  $q_{ph}$ , of an unglaciated particle depends non-linearly on the bed gradient ( $\nabla b$ ):

$$q_{ph} = - \frac{K_h \cdot \nabla b}{1 - \left(\frac{|\nabla b|}{S_c}\right)^2}, \quad (8)$$

where  $K_h$  is the hillslope diffusion coefficient.

Glaciated particles can be incorporated into the ice either from the ice surface, for supraglacial debris, or from the ice-bed interface by basal quarrying. The horizontal velocity of each glaciated particle is computed as a function of their depth within the ice  $z_p$ , relatively relative to the ice surface. Because iSOSIA is a one-layer depth-integrated model, the horizontal velocity depth-profile is computed following Glen’s flow law (Glen, 1952). We follow Rowan et al. (2015) in assuming that, due to the ice viscosity, the horizontal ice velocity decays as a fourth-order polynomial of the ice thickness:

$$u_p(z_p) = \frac{5}{4} [1 - z_p^4] \bar{u} + u_b, \quad (9)$$

where  $\bar{u} = \bar{u}_d + u_b$  is the average velocity of the ice, with  $u_b$  the basal ice speed and  $\bar{u}_d$  the average velocity due to the internal deformation of the ice which is approximated as a tenth-order polynomial of the local ice thickness, the bed and ice surface gradients, as well as its curvature (Egholm et al., 2011). We stress again that we neglect the transport of particles by meltwater and focus only on the ice and hillslope processes. Velocity profiles for glaciated and unglaciated particles are depicted in Fig. (S2).

The burial depth of particles ( $z_p$ ) within the ice is expressed relative to the ice surface (i.e.  $z_p = 0$  at the ice surface and  $z_p = 1$  at its base, Fig. 1), and computed according to the mass balance:

$$\frac{\partial z_p}{\partial t} = \frac{z_p \dot{M}_b - (1 - z_p) \dot{M}_s}{H}, \quad (10)$$

where  $\frac{\partial z_p}{\partial t}$  is the change in burial depth of a particle through time,  $\dot{M}_b$  and  $\dot{M}_s$  are the surface and basal melting at time  $t$ , respectively, and  $H$  is the ice thickness. Relative to the ice surface elevation, particles are moved downward according to the accumulation rate (in the accumulation zone  $\dot{M}_s < 0$ ), or upward with the lowering of the ice surface due to melting (in the ablation zone  $\dot{M}_s > 0$ , Fig. 1).

In the experiments presented in the following sections, detrital particles are sampled throughout the frontal moraine, defined as the glacier tongue (Fig. 1 and Fig. 5d). As vertical mixing of sediment has been reported in some glacier fronts (Enkelmann et al., 2009; Grabowski et al., 2013; Enkelmann and Ehlers, 2015), we sample particles independently of their vertical position within the ice thickness to infer detrital age distributions.

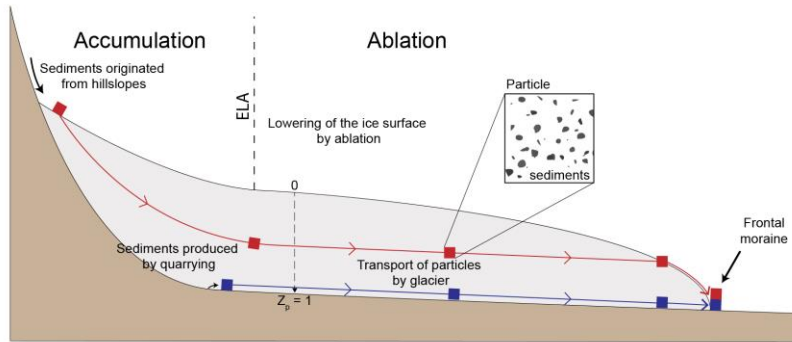


**Figure 1:** Particle transport by ice. Particles originated from hillslopes enter to the glacier system from the surface ( $z_p = 0$ ), whereas particles produced by the ice erosion are incorporated in the basal ice ( $z_p = 1$ ). The transport of glaciated particles follows the ice flow pattern from the sources to the frontal moraine. ELA is the equilibrium line altitude.

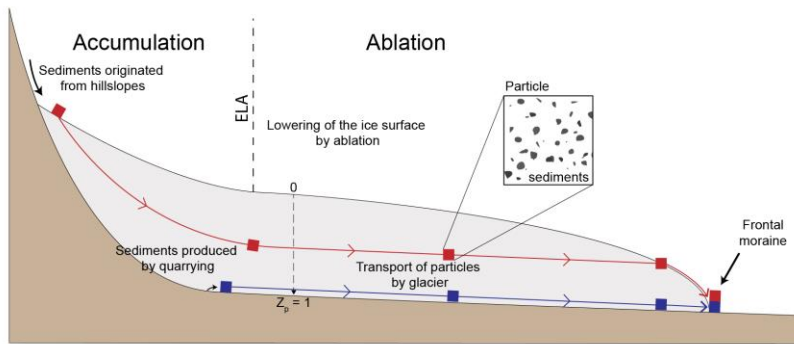


**Figure 1:** Particle transport by ice. Particles originated from hillslopes enter to the glacier system from the surface ( $z_p = 0$ ), whereas particles produced by the ice erosion are incorporated in the basal ice ( $z_p = 1$ ). The transport of glaciated particles follows the ice flow pattern from the sources to the frontal moraine. ELA is the equilibrium line altitude.

### 2.3 Modelling the Tiedemann glacier

Our main goal is to investigate the influence of ice-erosion-sediments sources and transport by ice on the shape of detrital SPDFs: at the glacier front. We present our modelling approach using the Tiedemann glacier catchment (Coast Mountains,

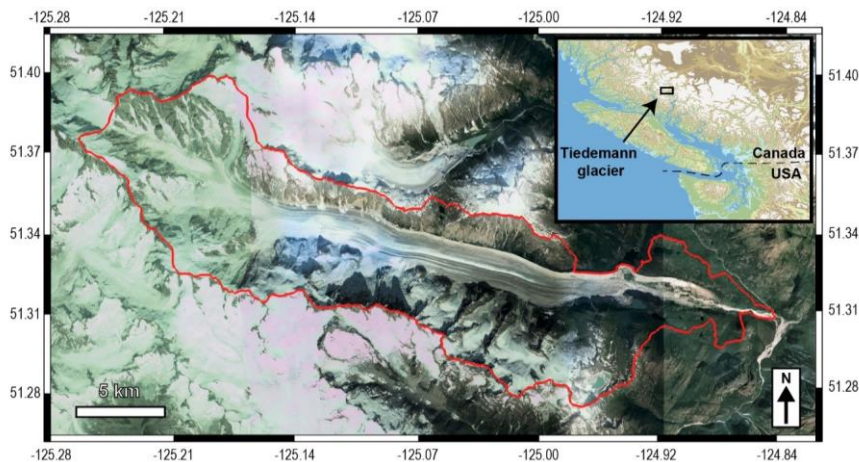


**Figure 2:** Satellite view of the Tiedemann glacier, British Columbia, Canada. The red contour represents the catchment area. The inset shows the regional location, in the Coast Mountain range, Canada. Note the dominantly linear pattern of sediments transport (image from ©Google Earth, Maxar Technologies; inset map with data from Jarvis et al., 2008).

British Columbia, Canada, Fig. 2) as a reference case-study. This region has been previously studied using detrital and in situ thermochronology (Ehlers et al., 2015; Enkelmann and Ehlers, 2015). Moreover, the Tiedemann glacier has simple morphological characteristics with a linear main glacial valley and small-extent tributary glaciers. Results of the simulations, We calibrated our iSOSIA model mimicking the Tiedemann glacier, performed with iSOSIA are tested by a trial-error process. We varied climatic, ice and hydrological parameters ( $dT_a$ ,  $C_s$ ,  $M_{acc}$  and  $k_0$ , see Table S1) and compared the resulting mean ice thickness and location of glacier tongue against the results of the ITMIX experiments (Farinotti et al., 2016; Farinotti et al., 2019) that predicts thickness of many glaciers around the world. The results of these calibration tests are shown in supplementary Fig. (S3). The reference iSOSIA, and thus the Tiedemann glacier model is presented in (Fig. (3S3)). To produce synthetic detrital age distributions resulting from this reference-model, we consider restrict the glacier to be in steady-state and impose a constant topography (i.e. erosion produces particles but no topographic changes). We stress that our goal is not to fit the dynamics of the actual Tiedemann glacier, which is in a phase of retreat (Tennant et al. 2012). Rather, we ask how surface processes affect the shape of detrital SPDFs in a simple case of constant and steady transport and erosion within a glaciated catchment.

The elevation of the Tiedemann glacier catchment ranges from 363 to 3920 m, for a total local relief of 3557 m. The resulting maximum ice thickness is 454 m with a mean ice velocity of  $13.2 \text{ m yr}^{-1}$ , and a range of 0 to  $109.2 \text{ m yr}^{-1}$  (Fig. 3), which are characteristic of Alpine glaciers (Benn and Evans, 2013). The mean ice velocity of the ice appears to be mainly controlled by the basal sliding speed, which in turn is influenced by the shear stress on the bed and the distribution of open-

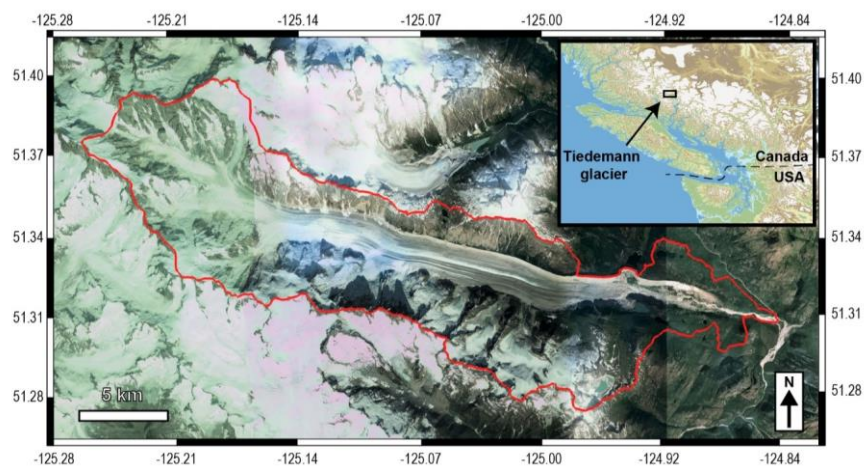


**Figure 2:** Satellite view of the Tiedemann glacier, British Columbia, Canada. The red contour represents the catchment area. The inset shows the regional location, in the Coast Mountain range, Canada. Note the dominantly linear pattern of sediments transport (image from ©Google Earth, Maxar Technologies; inset map with data from Jarvis et al., 2008).

cavities the effective pressure (Fig. S4). This results in two main partregions of relatively high velocities ( $\sim 60 \text{ m yr}^{-1}$ ) located at  $\sim 7 \text{ km}$  and  $\sim 14 \text{ km}$  in the glacier latitudinal coordinates (Fig. 3c).

#### 2.4 Synthetic ages and production of probabilitydetrital age distributions

To produce detrital SPDFs we need to specifyset the bedrock or in situ age distributions. Here, we predict ages for two thermochronological systems: the apatite (U-Th)/He (AHe) and apatite fission track (AFT). For the two systems To this end, we consider the age-elevation relationship inferred profiles from the bedrock data two low-temperature systems presented by in Enkelmann and Ehlers (2015) (AFT ages), and from Ehlers et al. (2015) for the Tiedemann glacier area (AHe ages, Fig. 4a). We use these as the basis of the bedrock age distribution in the catchment assuming assume that true AHe and AFT ages in the bedrock at a given elevation are given by the age-elevation relationship. In practice, thermochronological analysis on a single-

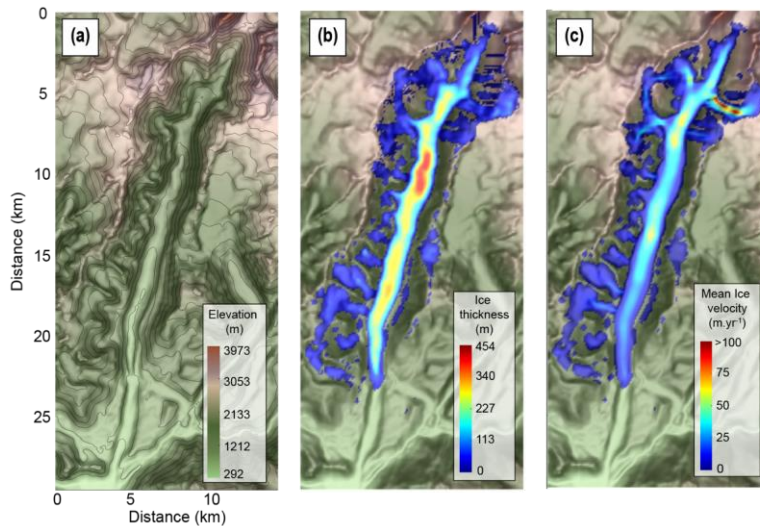


**Figure 3:** Characteristics of the Tiedemann glacier model. (a) The underlying topography, (b) the ice thickness, and (c) the mean ice velocity. The mean ice thickness has been calibrated with the ITMIX experiments (see supplementary)

10 grain is presented as an age and its associated uncertainty. Thus, the measured age can be considered as a noisy sample of the

true age. To produce a SPDF, we simulate this process for the detrital grain ages by adding random noise to the true ages, and assume ~~these~~the detrital grain ages are not modified during transport and deposition.

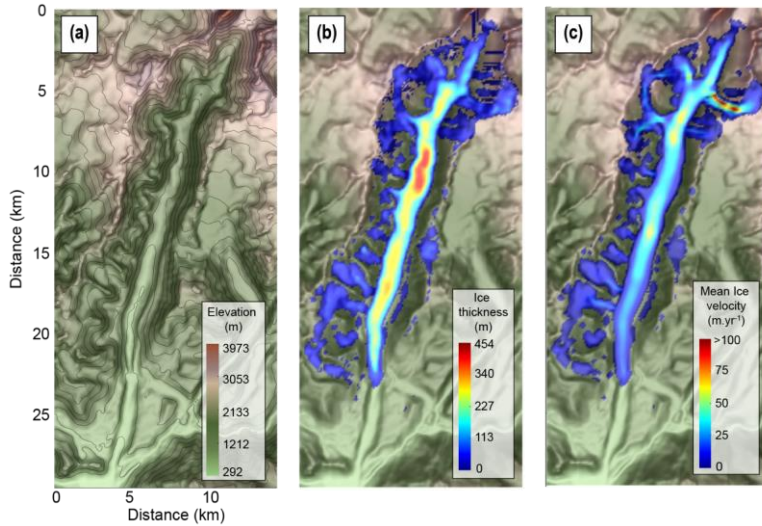


**Figure 3:** Characteristics of the Tiedemann glacier model. (a) The underlying topography, (b) the ice thickness, and (c) the mean ice velocity. The mean ice thickness has been calibrated with the ITMIX experiments (see Fig. S3)

In Ehlers et al. (2015), AHe bedrock ages and ~~therefore~~thus detrital data ~~appear to~~ have relatively high uncertainties (~21%). However, we stress here that one of our goals is to assess the effect of age uncertainty on the interpretation of SPDF, ~~and not~~  
5 ~~to reproduce the SPDFs presented in Enkelmann and Ehlers (2015); then we chose to apply lower uncertainty for the synthetic AHe ages.~~ For this reason, we adopt uncertainties of 10% for the synthetic AHe ages sampled from the age-elevation profile. This is similar to the typical reproducibility in aliquots of single grain ages (e.g. ~6% Farley and Stocki, 2002).

The AFT data from Enkelmann and Ehlers (2015) show >30 % relative uncertainties. We generate synthetic AFT ages following an approach similar to Gallagher and Parra (2020). We use the external detector method (EDM) age equation (e.g.  
10 Hurford and Green, 1983) to calculate the ratio of the spontaneous and the induced track density ( $\rho_s/\rho_i$ ) corresponding to a given AFT age in the age-elevation profile. To allow for the effect of variable high uncertainties, we simulate the range of relative error of the Enkelmann and Ehlers (2015) study: ~~To do this, we by~~ randomly sample the published values of  $N_s + N_i$  (i.e. the sum of the number of spontaneous and induced tracks) ~~from the data of Enkelmann and Ehlers (2015).~~ We then use a

binomial distribution with parameter  $\theta = \frac{\rho_s/\rho_i}{1 + \rho_s/\rho_i}$  to sample  $N_s$  values, corresponding to the number of spontaneous tracks,  
15 given the sampled value of  $N_s + N_i$  (see Gallagher, 1995; Galbraith, 2005). With the randomly sampled value of  $N_s$ , conditional on the sampled value of  $N_s + N_i$ , we easily obtain a value for  $N_i$ . We can estimate a “noisy” AFT age and relative error from

the sampled  $N_s$  and  $N_i$  values by using the EDM equation. For both the AHe and AFT systems, we attribute for each particle a single age and uncertainty in accordance with its source location elevation.

The probability age distributions are then produced by using Gaussian kernel density estimate (Brandon, 1996; Ruhl and Hodges, 2005) with the mean and standard deviation equal to the age and error for both the AHe and AFT ages, following

$$SPDF_{t_k} = \frac{1}{N_p} \frac{1}{\alpha \sigma_{t_k} \sqrt{2\pi}} \exp \left[ -\frac{1}{2} \left( \frac{t - t_k}{\alpha \sigma_{t_k}} \right)^2 \right], \quad (11)$$

$$SPDF_k = \frac{1}{N_p} \frac{1}{\alpha \sigma_{t_k} \sqrt{2\pi}} \exp \left[ -\frac{1}{2} \left( \frac{t - t_k}{\alpha \sigma_{t_k}} \right)^2 \right], \quad (11)$$

where  $N_p$  is the total number of sampled particles (i.e. ages),  $t$  is the range of ages in which we compute the SPDF,  $t_k$  the age of a particle considered,  $\sigma_{t_k}$  the associated age uncertainty, and  $\alpha = 0.6$  is a scaling factor that handles the resolution and the

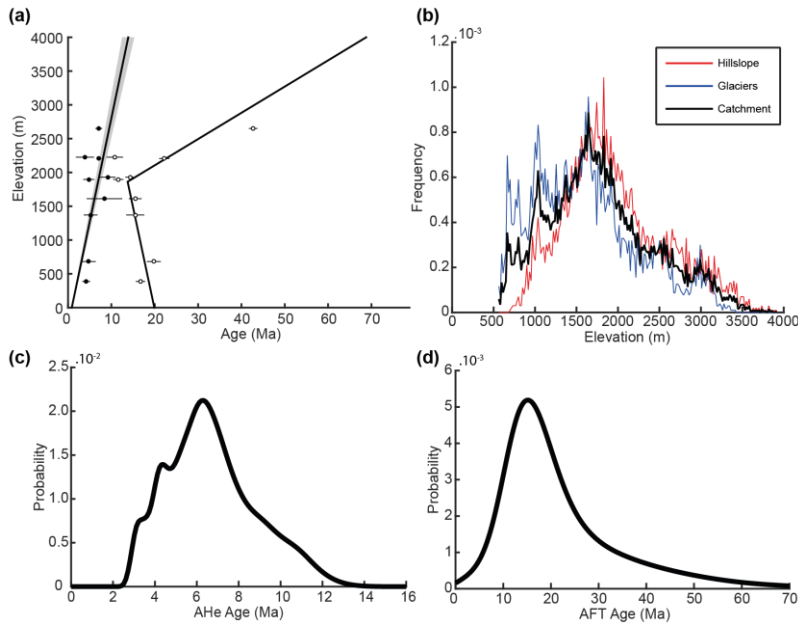


**Figure 4:** Synthetic bedrock thermochronological age distributions for the Tiedemann glacier model. The age-elevation profile for the two thermochronological systems AHe and AFT (a). Black and white circles represent the bedrock AHe and AFT ages from Ehlers et al., (2015) and Enkelmann and Ehlers (2015) respectively. Solid black lines are the best fit solution for the data. Shaded area for the AHe age-elevation show the 10% uncertainty considered for AHe ages. The catchment hypsometry frequency as well as glaciers and hillslope hypsometry frequencies are presented in (b). The bedrock AHe distribution considering 10 % relative uncertainties and bedrock AFT distribution with >30% relative uncertainties are shown in (c) and (d) respectively.

precision of age components in a SPDF (Brandon, 1996). To compare age distributions, we also define a cumulative synoptic probability density function, which is simply the cumulated sum of the SPDF:

$$CSPDF = \sum_{j=0}^{N_p} SPDF_j \quad (12)$$

Given the relatively high number of particles within the frontal moraine (i.e.  $> 10^6$ ) and to mimic real detrital sampling, all the detrital SPDFs presented in the following sections are produced by randomly sampling 105 particles from the total, independently of their source origin (Sections 3.2, 3.3 and 3.5) or accordingly (Section 3.4). This is similar to the proposed minimum number of ages to adequately resolve a component representing  $>5\%$  of the total detrital population (Vermeesch, 2004). We repeat this sampling process 10-thousand,000 times, storing the resulting SPDFs. From all of these detrital SPDFs, we compute the mean detrital SPDF and present the range of inferred detrital distributions.

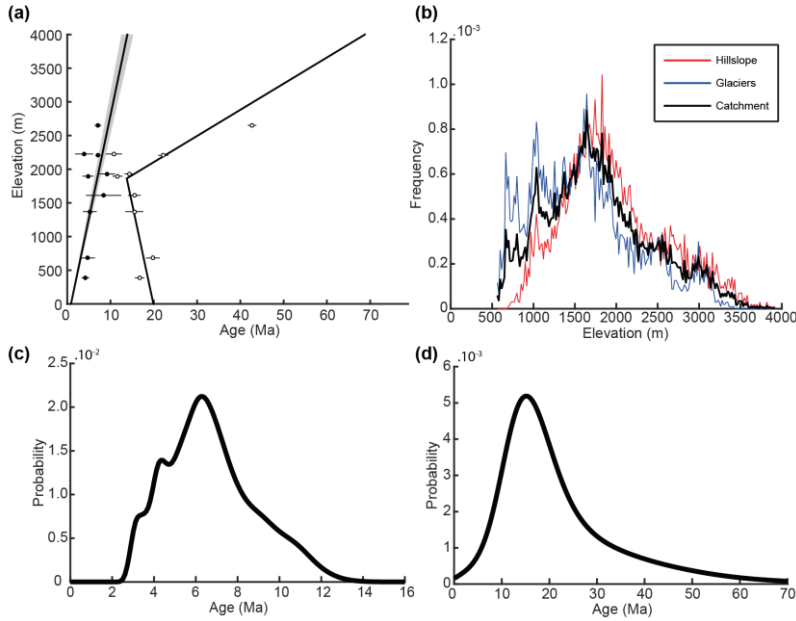


**Figure 4:** Age-elevation relationship for the two thermochronological systems AHe and Aft (a). Black and white circles represent the AHe and Aft ages from (Ehlers et al., 2015). Solid black lines are the best fit solution for the data. Shaded area for the AHe age-elevation show the 10% uncertainty considered for AHe ages. The catchment hypsometry frequency as well as glaciers and hillslope hypsometry frequencies are presented in (b), and bedrock AHe and Aft distributions are in (c) and (d), respectively.

### 3 Results

#### 3.1 Ideal detrital age distributions

The ~~ideal detrital~~bedrock age distributions for the two thermochronological ~~systems~~systems, AHe and AFT, ~~are presented in~~ (Fig. 4c-d). ~~These are ideal in the sense that they~~ represent the ~~bedrock~~ideal detrital age ~~distribution~~distributions if we sample  
5 the total catchment uniformly, ~~with noise. (allowing for the added to the true ages sampled from the age elevation profile. noise).~~  
In the subsequent text, we refer to these ideal detrital age distributions as the bedrock distributions. The bedrock AHe SPDF shows a major peak ~~at~~ ~6.3 Ma with two youngest smaller peaks ~~at~~ ~3.3 and ~4.3 Ma, and an older one ~11 Ma. The ~~form~~shape of this SPDF mimics the hypsometric curve (black curve, Fig. 4b) which is expected with a uniform production of sediments and a linear age-elevation relationship. The AFT SPDF shows a single major peak ~~at~~ ~15~16 Ma and the form does  
10 not mimic the hypsometric curve. This reflects partly the form of the age-elevation relationship, in which the ages below 2000 m (Fig. 4a) are similar, limiting the ability to resolve a unique relationship of age and elevation. We also note that, due to the high uncertainty, the probability to have an AFT age equal to zero is non-null.

#### 3.2 Transport of detrital particles

~~We~~Here, we investigate the kinematics of particles ~~within~~in our reference model for the Tiedemann glacier at the equilibrium  
15 state. ~~One~~To this end, we produce one particle ~~is produced~~in each cell of the model ~~at a specific time~~simultaneously (Fig. 5a) and ~~let particles to be~~ transported away, potentially to the glacier front (i.e. the frontal moraine) where they would ~~deposit~~be  
20 ~~deposited~~ (Fig. 5b-d). In this case, assuming we have reached steady state in terms of transport, differences between the final detrital and the bedrock SPDFs can only be related to the process of particle transport. ~~Figures 5b-d show the evolution of particle locations at 500, 1000 and 8500 years after the production of particles. Obviously, the pattern of particle transport is consistent with the ice velocity field (Fig. 3c).~~

~~Figure 6 summarizes~~We investigate the evolving contribution of ~~particles from different~~particle source locations to the detrital age distribution within the frontal moraine. ~~First characteristic we point out is , and to the inferred detrital age distributions~~ (Fig. 6). Particles are sampled independently of their source origin (hillslope vs glacial, Fig. 5a). According to our model, the minimum time, ~~~500 years~~, required for a particle originated from elevated parts of the catchment (i.e. far from the glacier

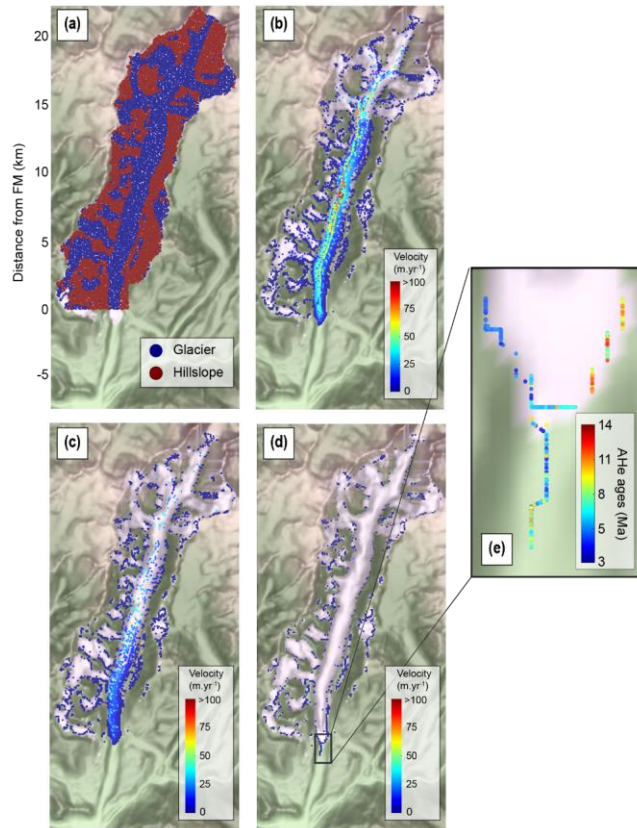


**Figure 5:** Kinematics of particles transport. Particles have been uniformly produced across the catchment and transported. (a) Sources of particles, red dots and blue dots are particles originated from hillslope and glacier at the beginning of the model simulation, respectively. (b) Particles velocity at time = 500 yr. (c) at time = 1000 yr. and (d) at time = 8500 yr. AHe ages in the frontal moraine (FM) are shown in (e) and see inset in (d).

front) to reach the frontal moraine, is ~500 years (Fig. 6a, pink curve). Furthermore, the proportions of particle source locations in the frontal moraine becomes nearly constant after ~1500–2000 years (Fig. 6a). After 8500 years, some particles are still close to their sources (Fig. 5d). We find that only 44% of the initial particles have reached the front of the glacier and the frontal moraine (Fig. 6b, black curve, and Fig. S5a). The other 56% is trapped upstream, with a large part of them resting in a lateral moraine (Fig. 5d and 6b, blue curve) or on the side of small tributary glaciers having very slow velocities (i.e.

< 1 m yr<sup>-1</sup>, Fig. 3c). These low velocities seem to result from a morphodynamic feedback ~~whereas~~ the slope of tributary glaciers that carry the remaining particles is close to zero in the direction of sliding (Fig. S5b). This could, in turn, be related to the location of the ELA (Fig. 6b). As the number of particles within the frontal moraine does not increase significantly after 2000 years of simulation (i.e. reaching around 37% of the total number of initial particles, see Fig. S5a), we consider the ~~steady-~~  
5 ~~state-of~~ detrital SPDF to ~~be~~have reached ~~at~~steady-state by this time.

Figure 5e shows the spatial distribution of AHe ages within the frontal moraine after 8500 years, while Fig. (6c) shows the

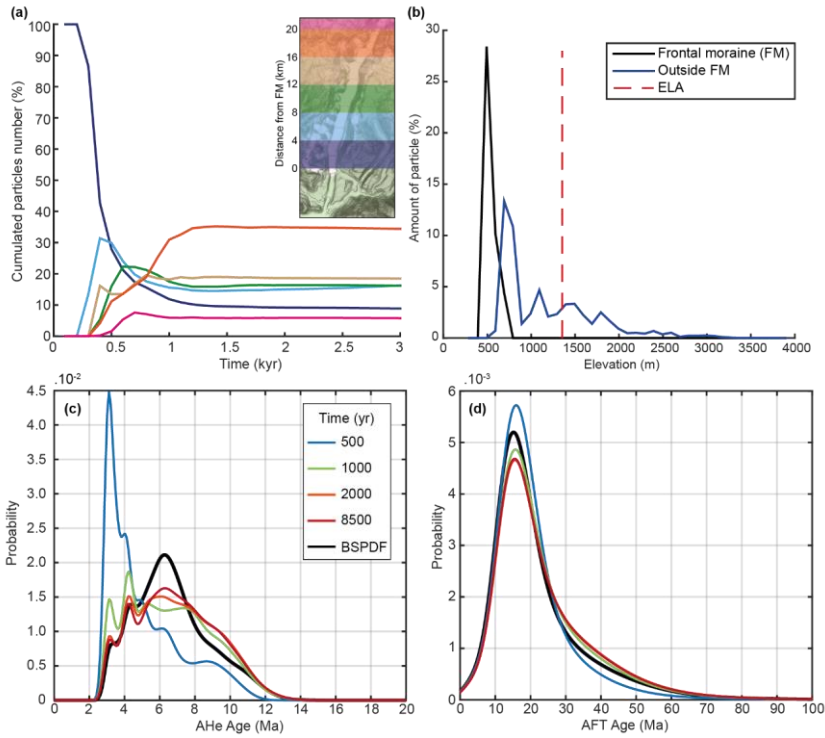


**Figure 6:** Transient evolution of particle sources and detrital thermochronological age distributions in the frontal moraine. (a) Cumulative contribution of source locations for particles. (b) their distribution with elevation after 8500 years of transport. (c) and (d) show the transient evolution of the detrital thermochronological age distribution in the frontal moraine for AHe and AFT systems respectively. BSPDF: Bedrock SPDF.

transient evolution of the mean detrital probability AHe age distribution (SPDFs) in the frontal moraine and also the bedrock SPDF. For the detrital SPDFs, we

We observe a relative decrease of young ages (blue curves) in the detrital SPDFs (Fig. 6c-d) with time during the transient phase, reflecting the progressive arrival at the frontal moraine of older ages coming from upstream and elevated parts of the catchment (see Fig. 4a and Fig. S6 for spatial bedrock age distributions). The formshape of detrital SPDFs reaches a steady-state around 4000-2000 years of simulation (red and orange curves).

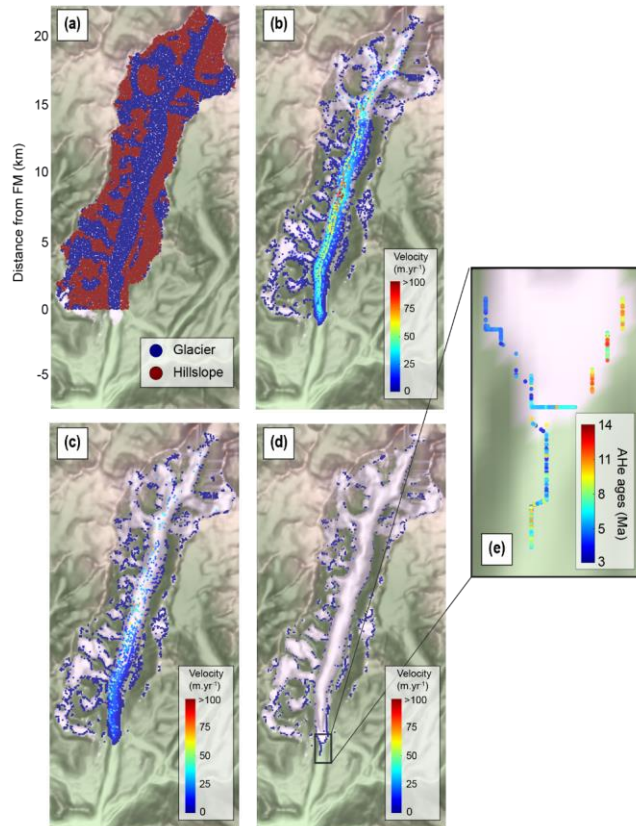


**Figure 5:** Example of particle transport. Particles have been uniformly produced across the catchment and transported. (a) Sources of particles, (b) particles velocity at time = 500 yr, (c) at time = 1000 yr, and (d) at time = 8500 yr. AHe ages in the frontal moraine (FM) are shown in (e) and see inset in (d).

Focusing on the steady-state The final form of the  $\Delta\text{He}$  detrital AHe SPDF (i.e. red curve), we can note differences with bedrock SPDFs (i.e. black curves). Indeed, this shows a lower age peak  $\sim 6.3$  Ma age peak has a lower relative proportion than in the bedrock SPDF. We also observe and a larger proportion of ages between 8 and 12 Ma in the detrital SPDF than in compared to the bedrock SPDF. The two youngest age peaks, at  $\sim 3.3$  and  $\sim 4.3$  Ma, in the detrital SPDF are however well represented in close to those of the detrital bedrock SPDF. This suggests Thus, the results suggest that the ice transport transports and deposit deposits mid-range ages, around 6 Ma (i.e.  $\sim 1500$ - $2000$  m), higher in the catchment.

For the AFT system (Fig. 6d), the peak age at ~16 Ma is similar for the detrital and bedrock distributions, but the magnitude of the final detrital age distribution peak ~16 Ma is also lower than that of the corresponding peak for bedrock age distribution.

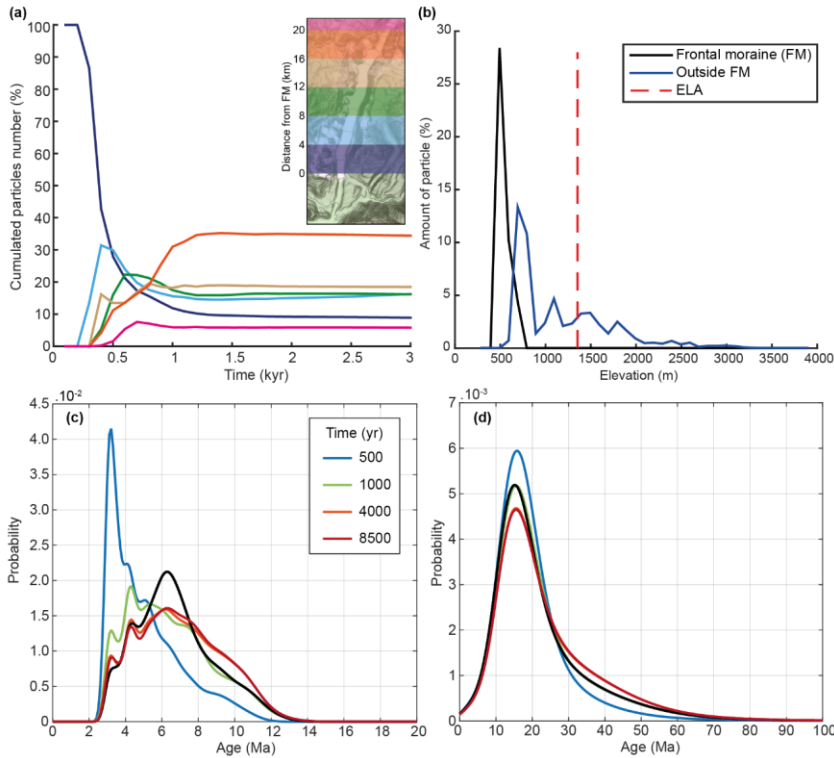


**Figure 6:** (a) Cumulative contribution of source locations for particles in the frontal moraine, (b) their distribution with elevation after 8500 years of transport. (c) and (d) show the transient evolution of the detrital thermochronological age distribution in the frontal moraine for AHe and AFT systems respectively. Black curves represent the bedrock (ideal detrital) age distributions of each of the two systems.

The relative contribution of old ages (> 25 Ma) is a little higher in the detrital SPDF, but for ages younger than 10 Ma, the distributions are similar. The differences suggest that ice transport also transports and deposit/deposits sediments mostly originated/originating from; 1000-2000 m in this case. We note that, the transient detrital SPDF at 1000 years (green curve, Fig. 6d) best matches the bedrock curve.

### 3.3 Detrital signature under uniform catchment erosion

~~In this section, Our model shows that more than half of the particles may not reach the frontal moraine. Consequently, we want to assess how the discrepancy between the detrital age distribution and the bedrock SPDF evolves if we consider a model with continuous production of particles (i.e. uniform erosion set at) across the catchment. To this end, we force the erosion rate to be  $1 \text{ mm yr}^{-1}$  in each cell of the Tiedemann glacier catchment (Fig. 7a), particles are then- This is within the range of natural values and it allows a continuous production of particles while maintaining a reasonable simulation time (i.e. a particle is produced continuously (i.e. every 10 years) in each grid cell (Fig-). In this section, no distinction is made between the two sources in the sampling process when building of detrital SPDFs. We stop the simulation 7a)- In contrast to the previous simulation, which was run over 8500 years, these models were terminated after 2000 years of simulation as the detrital SPDF in the frontal moraine is close to equilibrium (Fig. 4e).~~

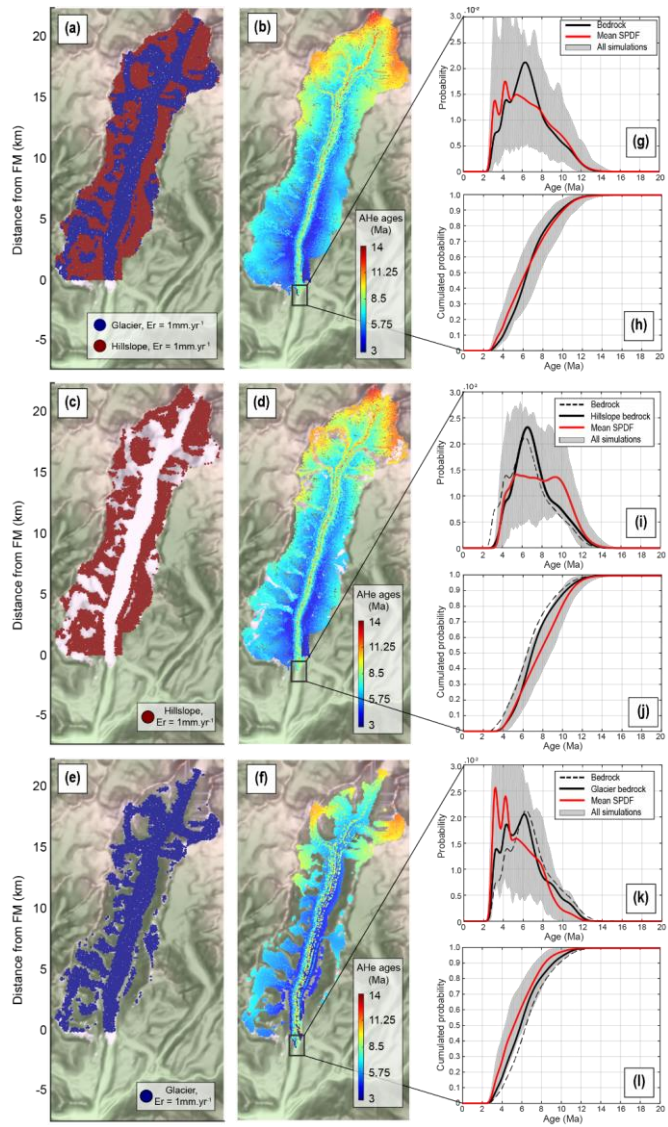


**Figure 7:** (a) Source of particles for the three models experiments: uniform sources of particles, (c) hillslope source of particles, and (e) glacier sources of particles, with  $E_r$  being the erosion rate. Their respective spatial AHe ages distributions after 2000 yr of particle transport are shown in b-d-f. Density plots and their cumulative distributions are shown in g-h, i-j, and k-l respectively. The black squares show the frontal moraine (FM) position.

This choice is also motivated by (6), and because the total number of particles increases rapidly which increases the computational efficiency reasons as the number of tracked particles in the model increases rapidly with increasing run time. Our aim is to estimate the form of the detrital SPDF at the glacier margin by sampling the frontal moraine, and to compare it with what is expected for the case of uniform erosion. Indeed, we expect that the detrital distribution will mimic the hypsometric curve (i.e. the bedrock SPDF). Here we will time. Here, we focus our analysis on the AHe system for clarity. The but the detrital SPDFs off the AFT system can be found in the supplementary material (Fig. S7). Figure 7a shows the spatial distribution of contributions from glacial and hillslope erosion processes, while the spatial distribution of detrital AHe ages after 2000 years of simulation is shown in Fig. (7b). The older ages are produced high in elevation, mainly by hillslope processes with local contribution from glacial erosion, whereas younger ages are produced by both hillslope and glacial erosion at lower elevation, according to the age-elevation relationship (Fig. 4a and Fig. S6a).

The detrital SPDFs resulting from the 10,000 sampling processes over the frontal moraine are summarised in Fig. (7g) where the range of calculated SPDFs is represented by the grey shaded area. Here, we qualitatively describe the resulting SPDFs. We First, we observe a large variability in of detrital SPDFs resulting from sampling 105 particles in the frontal moraine with a maximum at  $\sim 3$  Ma (Fig. 7c, 7g). The However, the bedrock age distribution is always included in the range of inferred detrital SPDFs. The Second, the mean detrital SPDF (red curve) however, represents the “true” detrital signal we expect to obtain by considering all the particles in the sampling site. This mean detrital SPDF shows some differences to the bedrock SPDF (black curve). In particular, the main age peak at  $\sim 6.3$  Ma of the bedrock SPDF is not obviously represented in the mean detrital differs from the previous model (Fig. 6c), in that the younger ages are over-represented with two high peaks (at  $\sim 3.3$  and  $\sim 4.3$  Ma); and also, there is an excess of older ages (8-11 Ma). However, mid-range ages  $\sim 5$  to  $\sim 8$  Ma are still under-represented compared to the bedrock SPDF. Looking at the cumulative probability age distributions (CSPDF), differences between the detrital CSPDF and the bedrock CSPDF are less clear, with the most obvious differences between 3 and 6 Ma.

SPDF similar to the previous model (Sect. 3.2), while the youngest age peaks at  $\sim 3.3$  and  $\sim 4.3$  Ma are over-represented. The proportion of old ages ( $> 8$  Ma) is similar to the bedrock SPDF. We therefore have a clear under-representation of ages ranging from  $\sim 5$  to  $\sim 8$  Ma. Looking at the cumulative distributions of age probability (CSPDF), we see minor differences between the detrital CSPDF and the bedrock CSPDF, with the most obvious differences between 3 and 6 Ma.

The results for the AFT ages (see SPDFs (Fig. S7a-b and S7g-hS7) show a similar tendency in under-represented representing mid-age peak although ages ( $\sim 16$  Ma) but much less pronounced, with a maximum difference between with the detrital and bedrock SPDFs SPDF at  $\sim 12.3$  Ma and a smaller one at  $\sim 24.928$  Ma. The AFT bedrock and detrital cumulated age distributions show a maximal CSPDFs have a maximum difference at  $\sim 19.2$  Ma, but are similar overall. The results show that detrital SPDFs are similar shifted toward younger ages, and deviate from what is expected for the case of uniform sampling (i.e. we expect the bedrock SPDF). We assign this behaviour to the short total transport distance for such ages. Furthermore, the SPDF is more

informative on the effect of transport than the CSPDF that tends to smooth the signal. Finally, the quality of the results depends on the age uncertainty of the thermochronological system and on the age-elevation profile.

### 3.4 Detrital signature of glacier and hillslope sources

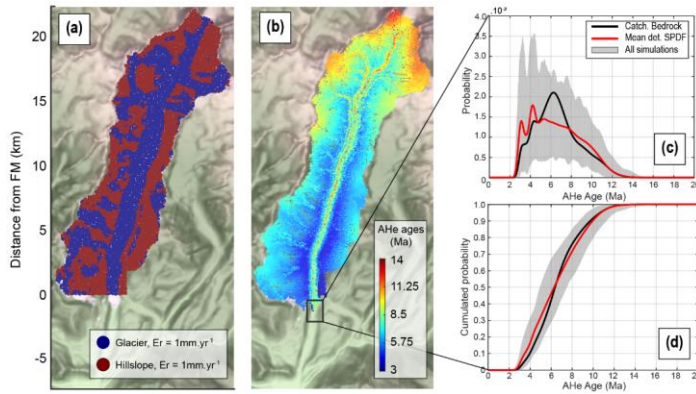


**Figure 7:** Spatial distribution of particles and detrital AHe age distributions within the frontal moraine. (a) Source locations of particles with  $E_r$  being the erosion rate. The spatial AHe age distributions of particles after 2000 yrs of transport (b). The detrital AHe age probability distributions (c) and their cumulatives (d). The grey shaded area represents the range of the inferred 10,000 detrital SPDFs from the sampling process. The black square in (b) shows the frontal moraine (FM) position.

5 ~~We~~To understand the form of the mean detrital SPDF above, we now assess the respective influence of the two main sources of eroded particles, the glacier and ice-free hillslopes, on the detrital SPDF, and glaciers. We first consider the ice-free hillslope sources (Fig. 7a). Within the frontal moraine we sample 7e). Particles are produced by the mean erosion rate set at 1 mm yr<sup>-1</sup>, as in the case of uniform erosion, but only particles originating that originated from ice-free areas are generated. The spatial hillslopes. Thus, the detrital AHe age distribution after 2000 years of simulation displays ages ranging range from 3.1 to 13.8 Ma (Fig. 7d) spanning ~96 % of the total age range shown by the age-elevation profile (i.e. from 2.7 to 13.8 Ma). Thus, we compute We calculate a new bedrock SPDF according to the hypsometric distribution of the sediment hillslope sources (black curve, Fig. 7i) that follow the hillslope hypsometry distribution (Fig. and the AHe age-elevation profile (Fig. 4). The 4b). The maximum age-range of inferred detrital SPDFs is in this case lower than the previous (Fig. 7i)-case (i.e. grey shaded area) but still remains important. The mean detrital SPDF shows a plateau-like signal from ~5 to ~9.5 Ma and differ from the hillslope bedrock SPDF, suggesting alone, uniform erosion for elevation that elevations from ~1400 to ~2500 m contribute in the same proportion to the particle budget in the frontal moraine. However, a comparison with the hillslope bedrock SPDF indicates that storage of sediment occurs for such elevations. Moreover, the hillslope mean detrital SPDF is shifted toward older ages (> 8 Ma) and excludes ages lower than 3.5 Ma as the hillslope sources de-erosion does not reach operate at the lower elevations showing such which have these young ages (Fig. 4b). Thus, the The hillslope mean detrital

CSPDF shows a maximum difference with the hillslope bedrock CSPDF around 8 Ma (thick black curve, Fig. 7j8b). Therefore, constraining the hillslope sources for the bedrock SPDF allows us to better identify the storage locations of sediments compared to the catchment bedrock SPDF (dashed curve, Fig. 7i-j8a-b).

The mean AFT detrital SPDF (Fig. S7jS8a) shows a similar tendency to over-representing old ages (> 25 Ma) and under-representing mid-range ages (~16 Ma) compared to the hillslope bedrock SPDF. However, the AFT-mean AFT detrital SPDF differs from the mean detrital AHe SPDF in that the bedrock AFT SPDF is always contained in the range defined by the shaded area and it does not show a plateau-like form. Indeed, two age peak components occur at ~16 Ma and at ~40 Ma. However, the detrital cumulative distribution (Fig. S7jS8b) is also shifted toward older ages,

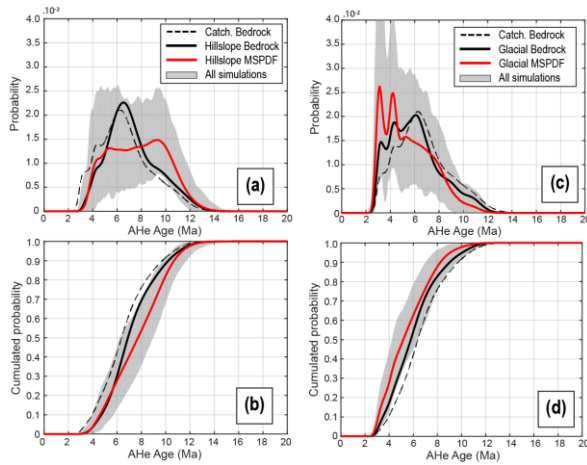


**Figure 8.** Detrital AHe age distributions of the frontal moraine, and their cumulatives, for models considering only ice-free hillslope sources (a-b) and glacial sources (c-d). The grey shaded area represents the range of the inferred 10,000 detrital SPDFs from the sampling process. MSPDF: Mean Synoptic Probability Distribution.

with a maximum difference at 24.5 Ma. This difference between the AHe and AFT age distributions is due to the different age-elevation relationships with lower spatial age resolution for the AFT system (Fig. 4a). Overall, the hillslope SPDFs reveal that the relevant source region ages tend to have older ages for both AHe and AFT, which is in accordance with the hillslope hypsometric distribution (Fig. 4b).

We now consider particles originated from the glacier source-glacial sources (Fig. 7e7a), which we define to be all the ice-covered areas. The associated detrital AHe ages range now from 2.7 to 12.1 Ma, according to the hypsometric distribution of glacial source part of the age-elevation profile (Fig. 4), spanning the first ~85% of the total age range of the catchment. The maximum age reflects the maximum elevation reached by the ice (i.e. ~3420 m). As previously, we compute a new bedrock SPDF according to the glacial source distribution (black curve, Fig. 7k) that is also in accordance

with the glacial hypsometric curve (Fig. 8, 4b). The detrital SPDFs ~~shows~~, representing particles of glacial origin in the frontal moraine, show a maximum range of inferred SPDFs at  $\sim 3.3$  Ma (grey shaded area, Fig. 7c, Fig. 8c). We relate this range to the constant 10% relative age uncertainty applied, as the range of inferred detrital SPDFs tend to increase with younger ages and younger ages have smaller absolute uncertainties. Compared to the glacial bedrock SPDF, the mean glacial detrital SPDF of the glacier source over-represents young ages ( $< 4.5$  Ma), in contrast to the hillslope source as we might expect. Next, we observe a relative under-representation of ages at  $\sim 6.3$  Ma and for ages older than 8 Ma, consistent with a storage of sediments at mid-elevation. This is reflected in the cumulative detrital distribution (Fig. 7d), which is shifted towards younger ages and does not intersect the glacier bedrock cumulative distribution. The maximum difference between the two cumulative distributions is at 4.6 Ma.

The detrital AFT distributions-age distribution (Fig. 8, 4S8) show the same tendency in over-representing young ages (age peak at  $\sim 15.7$ – $16.5$  Ma) compared to the glacier bedrock distribution and by under-representing old ages ( $> 27.5$ – $28$  Ma). However, the differences are less pronounced. The cumulated distributions show a detrital CSPDF is also shifted toward younger ages, where the maximum difference at  $\sim 28$  Ma with the bedrock CSPDF is observed  $\sim 28$  Ma. We notice however a smaller difference between the detrital and the bedrock CSPDF distributions for the AFT than for the AHe system.

Overall, the differences are explained by the lack of results show that older ages incoming from mainly reflect hillslope sources and younger ages, the glacial sources, which is expected given the age-elevation profile and hypsometric curves of the two sources (Fig. 4b). However, they also show that estimation of the bedrock distributions of the sources helps better constrain the role of the ice transport, and also better identify the predominant source in the sediment at the sampling site.

### 3.5 Detrital signature using a landscape evolution model with non-uniform erosion

To illustrate how the last numerical experiment, we look at bedrock distributions of the sediment sources can help identify the dominant source signal at the detrital age probability distribution within the frontal moraine resulting from the sampling site, we consider now a model with non-uniform erosion. We use erosion laws presented in Sect. 2.1 with parameters listed in Table 1. This, which leads to a non-uniform model of the erosion (Fig. 8a) with pattern in Figure 9a. Eroded particles are thus a mixture of hillslope- and glacier-origin sources for particles. The parameters of the erosion laws were calibrated by a trial-error process to obtain a mean erosion rate over both source regions of  $1 \text{ mm yr}^{-1}$ ; for a more consistent comparison with the constant erosion rate models. Obviously, local deviations to variations occur locally about this mean value (e.g. maximum erosion rate is  $\sim 31 \text{ mm yr}^{-1}$ ) as shown by Fig. 9a) and the calculated standard deviations for the mean erosion rates for the hillslope and glacier sources are  $1 \pm 0.29$  and  $1 \pm 2.9 \text{ mm yr}^{-1}$  respectively, where the glacier erosion is more variable. Ice erosion pattern results. Variations in ice erosion result mostly from the distribution of effective pressure that controls the opening of cavities (Eq. 3 and Eq. 6) and therefore from the length on which the basal shear stress is applied (Eq. 1 and Fig. S1). Consequently, there are some ice-covered areas that do not erode at all. The range of detrital ages for the glacier-origin particles spans 9 Ma from 2.7 to 11.7 Ma, whereas those for the hillslope-origin particles range from 3.5 to 13.8 Ma (Fig. 8b).

reflecting both the sampling of the age-elevation relationship with higher elevation tend to be subjected to hillslope erosion, compared to glacier erosion that is mostly restricted to valley floors (Fig. 8a).

The mean detrital SPDF shows a large age peak  $\sim 5$  Ma, and a smaller one  $\sim 10$  Ma. The glacial bedrock distribution predominates for ages  $< 5.5$  Ma (Fig. 9c), suggesting a glacial source for the first age peak. This is confirmed by the high erosion rates located where the AHe ages are around 5 Ma (see Fig. 9a-b and Fig. S6a). Looking at the detrital distributions (Fig. 8c), we observe large differences between the mean detrital and the catchment bedrock SPDF. First, a single major age peak occurs at  $\sim 5$  Ma, suggesting a predominant glacier source at  $\sim 1500$  m. Second, an older age peak occurs at  $\sim 10$  Ma, thus reflecting mostly the hillslope source and elevation  $\sim 2800$  m (Fig. 8a). Very young ages ( $< 4$  Ma) are not represented as very low erosion rates ( $< 0.07$  mm yr $^{-1}$ ) of glacier source occur at low elevations. The corresponding mean detrital CSPDF

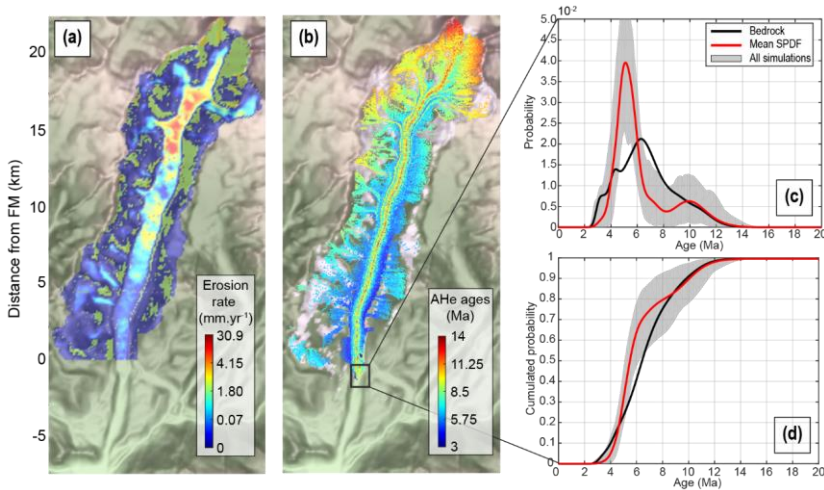


**Figure 8:** Non-uniform erosion model experiment, with the (a) erosion rate, (b) the spatial AHe age distribution, (c) the density and (d) cumulative distribution plots for the frontal moraine. The black square in (b) shows the frontal moraine (FM) location.

(Fig. 8d) shows a shift towards young ages compared to the bedrock CSPDF, the maximum difference between the two cumulative distribution being at 4.9 Ma. We also note that the bedrock CSPDF shows clear departure from the range of possible detrital CSPDFs at  $\sim 6$  Ma (grey shaded area, Fig. 8d), tracing a major glacier source contribution to the detrital SPDF of the frontal moraine.

The mean AFT detrital SPDF (Fig. S8e-d) The second age peaks (10 Ma) best match with the hillslope bedrock distribution, which would suggest a dominant hillslope source contribution. This assumption is also confirmed by the erosion rates  $\sim 1.80$  mm yr $^{-1}$  where AHe ages are  $\sim 10$  Ma (Fig. 9a and Fig. S6). The mean detrital SPDF also shows a low at  $\sim 7-8$  Ma that we

attribute to both the effect of storage at mid elevation (Fig. 6b) and the erosion pattern, as the relevant elevations are represented by small tributary glaciers with low erosion rates ( $<0.07 \text{ mm yr}^{-1}$ ). A similar comparison can be done with the CSPDFs (Fig. 9d), although the curves are smoother. Thus, taking into account the bedrock age distributions of the different sources increases the potential to discriminate these sources in a detrital sample. However, we stress that the bedrock distributions are based on the assumption of spatially uniform erosion across the catchment. Non-uniform erosion leads to different bedrock SPDF for the sources, and also different expected sediments source distributions.

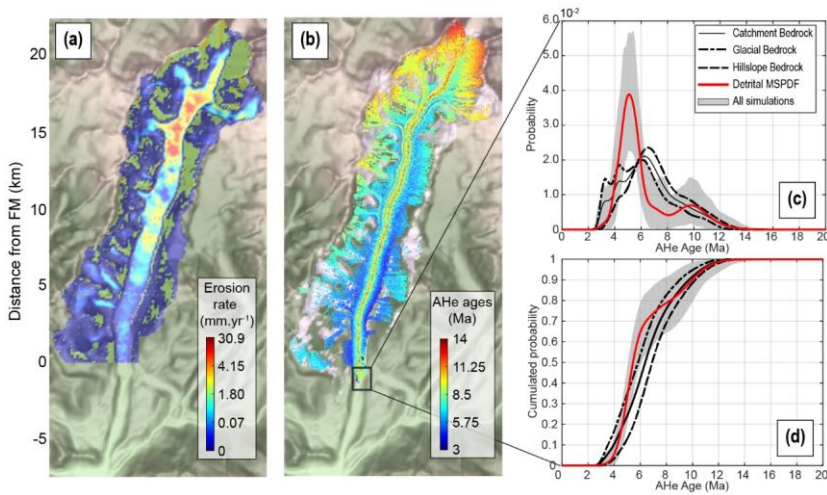


**Figure 9:** Non-uniform erosion model experiment, with (a) the erosion rate, (b) the spatial AHe age distribution of particles, (c) the detrital AHe age probability distributions and (d) their cumulative for the frontal moraine. The grey shaded area represents the range of the inferred 10,000 detrital SPDFs from the sampling process. The black square in (b) shows the frontal moraine (FM) location. MSPDF: Mean Synoptic Probability Distribution Function.

The mean detrital AFT SPDF (Fig. S9) is in agreement with a glacial source of particles for AFT ages  $\sim 16 \text{ Ma}$ , where the erosion rates are highest (Fig. S9a), but this is much less pronounced than for the AHe system. Moreover, it is difficult to make distinction between the two sources (hillslope vs glacier) for ages  $>30 \text{ Ma}$ , as the mean detrital SPDF closely match all the bedrock SPDFs. We relate this pattern to the large relative uncertainties (i.e.  $>30\%$ ) we considered for the AFT ages, that over-smooth the SPDF, especially for older ages. The mean detrital CSPDF shows no significant differences with the bedrock SPDF and bedrock CSPDF does not show departure from the range of possible detrital age distributions. This catchment bedrock CSPDF and suggests a uniform erosion across the catchment, which is in contradiction with contrast to the conclusion inferred from for the AHe system, that shows i.e. a major contribution of the glacier source. This difference is, due to the different age-

elevation relationships and age uncertainties between the two thermochronometers, ~~reducing in the case of the AFT system, reduces~~ the ability to track the source of particles. ~~In this case, the AFT detrital distribution is not able to resolve the different contribution of the two sources (hillslope and glacier), with AFT data in this example.~~

## 4 Discussion

### 5 4.1 Limitations of the particles transport model

It is important to note that the sediment particles in ~~the~~our model are passively transported ~~passively~~ and do not interact with the ice. For instance, the concentration of debris in the basal ice can influence the rheology of the ice and the friction of the bed, which both impact the ice flow (e.g. Hallet, 1981; Iverson et al., 2003; Cohen et al., 2005). Surface debris-cover can also shield the ice from solar energy and, in turn ~~reduce, reduces~~ the ablation rates and ~~increase~~increases the local mass balance of the glacier (e.g. Östrem, 1959; Kayastha et al., 2000; Rowan et al., 2015). As iSOSIA does not perform a full 3D computation of ice deformation, the horizontal velocity of particles is parametrized as a simple polynomial function (i.e. Eq. 9) of the average ice velocity (i.e. for englacial particles). Sediments can move vertically only by the accumulation of new ice or by melting, whereas natural particles can also move due to internal ice deformation, including thrusting and folding (Hambrey et al., 1999; Hambrey and Lawson, 2000). Surface debris may also fall in crevasses and therefore be incorporated in the basal ice (Hambrey et al., 1999).

~~Lastly, sediment transport by rivers and sub-glacial drainage is neglected in the model.~~

Additionally, our models omit debris comminution during transport. This process may have important implications for sampling strategies as block sized sediments formed by, e.g. quarrying, potentially originate close to the sampling site (i.e. have a short travel distance), but often are not sampled. This could bias detrital SPDFs, that are only representative of the sampled size fraction of sediments (mostly sand size) and thus sources located high in the catchment (i.e. larger travel distances). Lastly, sediment transport by rivers and sub-glacial drainage is neglected in the models presented here. However, it has been shown that a large part of basal debris can be evacuated by meltwater, on a seasonal timescale (Collins, 1996; Kirkbride, 2002; Swift et al., 2005; Delaney et al., 2018). Not allowing for this factor potentially impacts the transfer time of our sediment particles to the glacier front and we return to this point below. Additionally, water mixes sediments efficiently and may reduce the role of advective sediment transport in the ice. The role of sediment mixing by water has been investigated by Enkelmann et al. (2015) and they conclude that sampling the pro-glacial river (Ehlers et al., 2015) is similar to sampling through the ice-core terminal moraine, meaning that sediments in glacial outwash have a greater potential to be mixed by meltwaters. We emphasise that our simple particle transport model is a starting point for studying the behaviour of sediment transport by ice, and integration of other processes of transport should be considered in future studies.

#### 4.2 Effect of sediment transport by the ice

Despite the limitations mentioned above, some first-order insights related to ice dynamics can be identified. Firstly, we characterize the time to reach an equilibrium in terms of the relative proportions of particle sources in the frontal moraine of around 1500 years. This time to reach equilibrium is similar to the timescale of the variability of glacier dynamics observed in valley glaciers (e.g. Nussbaumer et al., 2007; Osborn and Luckman, 1988). This suggests that a detrital age distribution sampled from a glacial deposit like a frontal moraine may often reflect a transient case, with variable proportions of particle sources depending on the transport times (Fig. 6a). Thus, estimation of spatial erosion pattern can be biased based on the detrital SPDF (e.g. Firstly, our ice transport model for the Tiedemann glacier implies an equilibrium time in terms of the relative proportions of particle sources in the frontal moraine of the order of  $10^3$  years (~1500 years). This timescale is of the order of the characteristic timescale developed by previous studies (Johannesson et al., 1989; Oerlemans, 2001; Roe and O'Neal, 2009; Herman et al., 2018) and mainly reflects the glacier dynamics. Incorporating transport of sediments by meltwater, this timescale would probably reduce for glaciers with well-developed drainage systems, as large part of glacier basal debris seems to be evacuated by the subglacial drainage system (Collins, 1996; Kirkbride, 2002; Swift et al., 2005; Delaney et al., 2018). However, the types of debris forming frontal moraines vary from glacier to glacier. For instance, debris-covered glaciers are dominated by supraglacial debris that are mainly transported passively by ice (Benn and Evans, 2013). Terminal moraines of debris-covered glaciers are thus mainly built by a dumping process of debris from the ice surface, and thus reflect glacier dynamics, especially if the glacier remains stable for a long period of time (Sharp, 1984; Lukas, 2005; Hambrey et al., 2008; Benn and Evans, 2013). Moreover, some sedimentological studies on terminal and lateral moraines have shown limited amounts of glaciofluvial-related facies (e.g. Winkler and Matthews, 2010; Bowman et al., 2018; Ewertowski and Tomczyk, 2020), as it is the case for the Tiedemann glacier (Menounos et al. 2013). Therefore, the timescale for building the frontal moraine would strongly depend on (i) the availability of subglacial debris vs supraglacial debris, and (ii) the glacier dynamics. We recommend that future studies should focus on the timescales for building the terminal moraine, but we also highlight that, in some glacial areas, this timescale could impact the interpretation of detrital SPDFs from such glacial features, e.g. by reflecting a transient phase of sediment arrival (as shown in Fig. 6). Ehlers et al., 2015). For instance, one may conclude that erosion is focused at low elevations (i.e. based on the young age peak in Fig. 6e). Secondly, zones of slow ice flow, such as in small tributary glaciers, may act as sediment traps as shown by particles remaining in elevated areas after 8500 years of simulation. These zones of slow ice motion occur mostly around the ELA and are associated to low values of local topographic slope. This is consistent with the suggestion that glacial erosion is more efficient around the ELA (e.g. Egholm et al., 2009; Brozović et al., 1997; Anderson et al., 2006; Steer et al., 2012), which leads to limited local relief and slope around the ELA and in turn to limited ice sliding velocity. This also highlights the role of morphodynamic feedbacks in controlling, here by a trapping effect, the detrital distribution of thermochronological ages. Therefore, only ~44% of the total initial number of particles have reached the frontal moraine after 8500 years of transport (i.e. the maximum time of our simulation). The remaining ~About 25 % of the particles are stored in the lateral

moraine (Fig. 5d) and the ~~others remaining~~ ~31% are trapped at higher elevations, and therefore have residence times greater than 8500 years. ~~The robustness of the results presented so far to different parameters has been tested by varying the glacier size, and the hillslope diffusivity for particle transport. The results are presented in Sect. 2 of the supplementary materials. Overall, the conclusions are similar to those already discussed, and show equilibrium times for the frontal moraine of the same order, and around 53-60 % of the total sediments stored higher in the catchment,~~

To illustrate ~~in more detail~~ the effect of low velocities on transport times ~~in more detail~~, we compute the average transfer time as a function of source location for particles that reach the frontal moraine (Fig. 9~~10~~). The results show that the time required for a particle to reach the frontal moraine is ~~obviously~~ not simply proportional to the distance ~~between the moraine and with~~ the source location. Indeed, some particles formed near the frontal moraine may take more than 3000 years to reach the glacier front due to velocities close to zero (Fig. 9a, red dots, and Fig. 9b, blue dots)~~10~~. In contrast, some particles formed far from the frontal moraine have transfer times less than 1000 years due to averaged-velocities greater than 15 m yr<sup>-1</sup> (Fig. 9b~~10b~~). The proximity of the source to ice streams with high velocities explains this pattern of transfer times (Fig. 3c). ~~It is also illustrated in Figure 6a where we observe that particles originating 8 to 20 km from the frontal moraine arrive at the same time, and that the proportion of particles from 12-16 km evolves more rapidly than those from 8-12 km. It results that the~~The average transfer times for particles formed along hillslopes or glaciers are 1825.4 ± 1914.7 and 1084.9 ± 1014 yrs, respectively, but

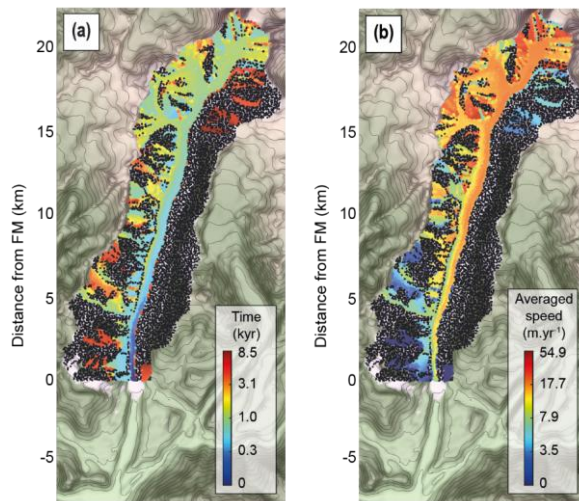


**Figure 9:** Characteristics of particles transfer to the frontal moraine, (a) the time needed for each particle to reach the frontal moraine; (b) their averaged speed. Black dots are particles that did not reach the frontal moraine (FM).

show high variability. This difference is controlled ~~41~~) by the longer average distance of the hillslopes to the frontal moraine,

Mis en forme : Police :Non Gras, Non Italique

15.26 ± 7.19 km, compared to glaciers, 13.85 ± 6.15 km, and 2ii) by spatial variation in ice flow velocities and storage of ~~sediments~~ sediments in small tributary glaciers. Overall, sediment transfer times of our models are strongly influenced by the spatial distribution of small tributary glaciers, suggesting implying an important control of the glacier sizesizes on the delivery of sediments to the main glacier transport system.

- 5 In the case of uniform erosion, ~~combined with and a linearsimple~~ combined with and a linearsimple relationship between thermochronological age and elevation (Fig. 4a), we expect ~~that~~ that the detrital thermochronological signal associated to each source mimies to mimic its associated hypsometric distribution. However, the resulting detrital SPDFs differ from that expected from the hypsometric distributions-  
(Fig. 7). The lack of the ages in the detrital SPDF corresponding to the peak observed ~1500-2000 m in the hypsometric curve, may be explained by (i) the storage of a major part of the sediments (i.e. 56%) outside of the sampling site, and (ii) by the  
10 patterns of transfer times for particles that ~~have reached the frontal moraine (Fig. 9)~~ reached the frontal moraine (Fig. 10). The generality of this conclusion is limited by our sediment transport model, as mentioned earlier, and the discrepancy observed between the detrital SPDFs and the expected distribution (i.e. bedrock SPDF) can be reduced for glacier with well-developed

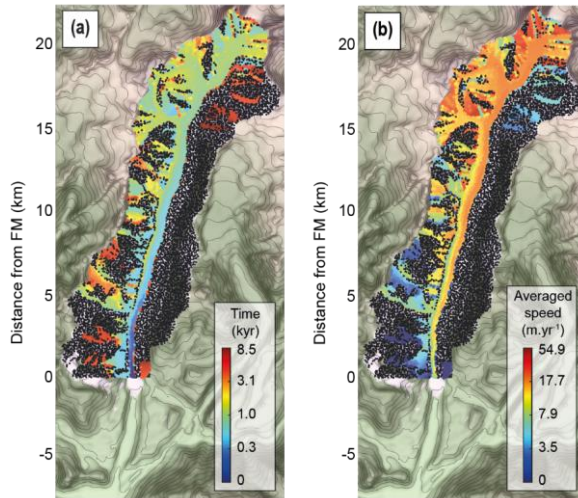


**Figure 10:** Characteristics of particles transfer to the frontal moraine. (a) the time needed for each particle to reach the frontal moraine; (b) their averaged speed. Black dots are particles that did not reach the frontal moraine (FM).  
subglacial drainage system.

### 4.3 The role of detrital sources: glaciers or hillslopes

Each According to our model for the Tiedemann glacier, each type of detrital source, i.e. hillslopes or glaciers, displays a different average hypsometry (Fig. 4b). Glaciers mostly represent valley floor while hillslopes mostly represent elevations greater than ~1800 m. We point out that hillslope sources contribute to older ages in the detrital SPDFs, as expected from the age-elevation profiles and the range of elevation of hillslope source (~700-4000 m). The glacial detrital SPDF (Fig. 78) reflects mainly the younger ages from the valley floor, and a lack of older ages as expected by in the range of elevation range occupied by glaciers (~530-3420 m). Moreover, depending on the erosion pattern, the proximity of the glacial source from the frontal moraine (<5 km) plays a role in the proportions of detrital age components, as the transfer times are lower (<300 years). The combination of the two source contributions is well illustrated in the case of uniform erosion through the catchment (Fig. 7), where the relative contribution of younger ages (glacier source) is reduced while the contribution of older ages better matches the bedrock distribution.

Characterizing When estimating glacial erosion rates from sediment flux measurements it is important to distinguish glacier-origin debris from supraglacial debris. Previous studies used cosmogenic nuclides concentrations (e.g. Guillon et al., 2015) or U-Pb ages (e.g. Godon et al., 2013) on sediments to discriminate between sources. Here, we tested a simple approach by characterizing the bedrock age distribution of different sources and compared them with the detrital age distribution. The model considering non-uniform erosion gave promising results for identifying contribution of different sources and the nature of particle transport allows us to better understand the mean detrital SPDF of sediment sources to the frontal moraine resulting from non-uniform erosion (Fig. 8)-9).

Despite identical averaged erosion rates for the two sources (i.e.  $1 \text{ mm yr}^{-1}$  for hillslope and glacier respectively), glacial erosion shows a more heterogeneous pattern than hillslope erosion. The resulting young age peak component ( $1 \text{ mm yr}^{-1}$ ), the resulting shape of the mean detrital SPDF (Fig. 8e, red curve) reflects a dominant is the result of higher local glacial contribution erosion rates compared to the frontal moraine. Indeed, local rates of more diffusive erosion by quarrying, from 0 to  $\sim 31 \text{ mm yr}^{-1}$ , is observed to be an order of magnitude greater than the maximum rate of hillslope erosion, from 0 to  $2.3 \text{ mm yr}^{-1}$  (Fig. 8a) on hillslopes. Therefore, the glacial process source locally produces more a high amount of sediment particles, with similar thermochronological ages, which are ultimately transported to the frontal moraine. This explains the high peak observed  $\sim 5 \text{ Ma}$  (Fig. 9) and the lower peak  $\sim 10 \text{ Ma}$  corresponding to hillslope sources. Furthermore, as glacial erosion is generally linked the proximity to the basal sliding speed (Eq. 6), we expect that glacial origin sources of particles to be close to ice streams presenting high depositional site of the sources with high glacier velocities, reducing in turn, the transfer time of such particles, also contributes to the magnitude of the age peak components observed in the detrital SPDF (Fig. 10).

Therefore, detrital SPDFs of glacial features like such as the frontal moraine are likely to over-represent glacial sources of sediments compared to hillslopes sources. Next if driven by locally high erosion rates. Finally, a large part of sediment particles produced on hillslopes originates from around 2800 m as illustrated by the older age peak component at  $\sim 10 \text{ Ma}$  (Fig. 8e). This peak occurs because the elevated areas are connected to the main glacier and thus have transfer times,  $\sim 800$  years, which

are of the same order of those where the local erosion rate is highest ( $\sim 31 \text{ mm yr}^{-1}$ , Fig. 8a). The spatial distribution of hillslope erosion rates in Fig. 8a confirms this source elevation (9c).

#### 4.4 Implications for detrital sampling strategies

A sampling strategy equivalent to ~~that~~ the one considered in this study (i.e. randomly sampling the entire frontal moraine) has the potential to capture ~~most of the bedrock age distribution. This is particularly true in the uniform erosion case where the mean detrital SPDF approximates well the bedrock SPDF. However, given the advective nature of particle transport by ice, we now consider the effect of more bedrock age components, as proposed in previous studies (e.g. Enkelmann et and Ehlers, 2015). To illustrate this effect, we now consider~~ different sampling strategies. We perform an additional experiment, with uniform erosion, where sampling occurs in four different regions of the frontal moraine (Fig. 10). The process of sampling is the same as for previous models, i.e. we randomly collect 105 particles within each region, produce a SPDF and repeat this

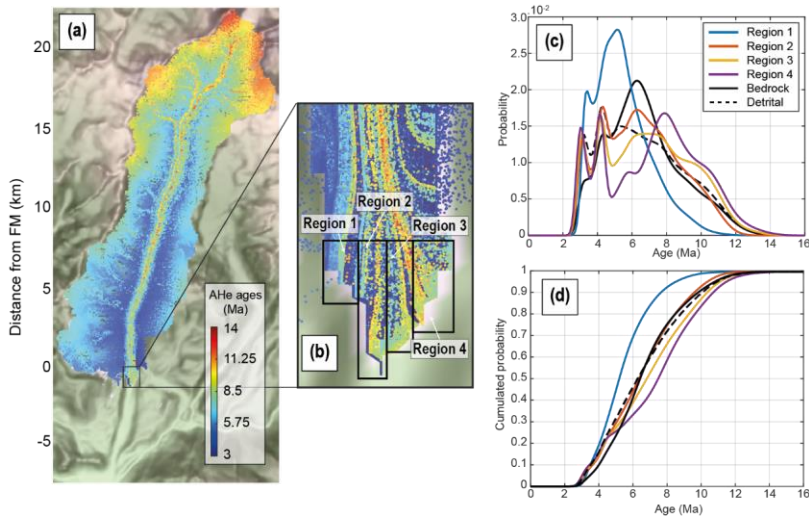


**Figure 10:** Detrital AHe age distribution of the five sites seen in (b, black squares) from the experiment considering uniform source of particles (a). The density plots and their cumulative distributions are shown in (c) and (d). The dashed black line is the mean detrital SPDF for the frontal moraine (FM).

process 10,000 times to infer a mean detrital SPDF. The resulting mean AHe detrital SPDFs and CSPDFs ~~are presented in~~ (Fig. 10). ~~We first observe a~~ 11 show significant variability ~~between the four detrital SPDFs.~~ Sampling region one (Fig. 10) mostly ~~represents captures~~ captures young ages ( $< 6 \text{ Ma}$ ) and therefore the glacier source. ~~The, while hillslope source sources, with older ages ( $> 6 \text{ Ma}$ ), is~~ are under-represented. Sampling ~~regions region~~ region two ~~and three, located in the closer to~~ closer to centre of the moraine,

include an older age component (>6 Ma), which leads to a better fit with the mean detrital SPDF obtained by sampling the entire frontal moraine. We note that the detrital SPDF of region two seems to better match

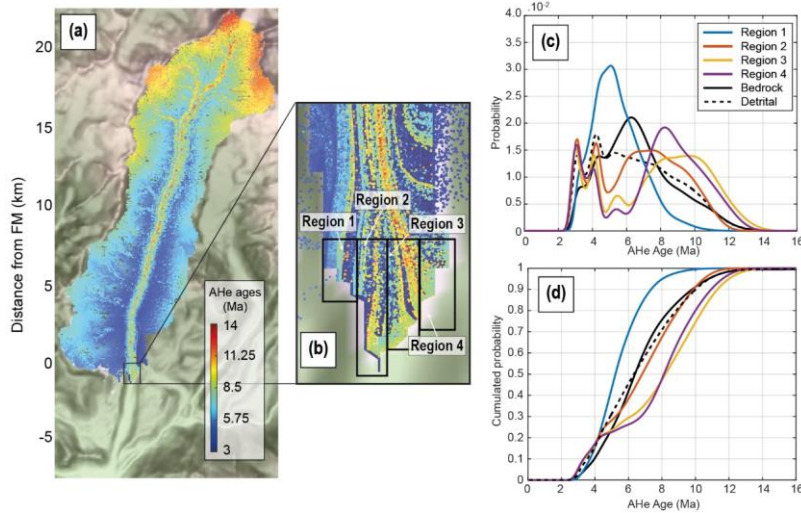


**Figure 11:** Detrital AHe age distributions of the five regions seen in (b, black rectangles) from the experiment considering uniform source of particles. Spatial distribution of particles with their AHe ages associated (a), with a zoom to the frontal moraine area in (b). The density plots and their cumulative distributions are shown in (c) and (d). The dashed black line is the mean detrital SPDF for the frontal moraine (FM).

CSPDFs confirm this similarity (see Table 1). However, the bedrock SPDF than the mean detrital SPDF, different sensitivity of these statistical tests complicates interpretation of these results. Finally, region the regions three and four shows a bimodal age distributions show similar distributions with an over-representation of young (<4 Ma) and old ages (>7.5 Ma), and a gap in mid-range ages (between 5 and 7 Ma) representing intermediate elevations (1500-2000 m). Focusing on the spatial distribution of detrital ages allows us to track the source of ages from the front of the glacier. We confirm that old Old ages (red dots in Fig. 10a11a-b) are mostly transported in the central part of the main glacier and deposited in the central part of the frontal moraine (regions two, three and threefour). An exception occurs with region regions three and four due to deviation of ice streamlines (Fig. 10b11b). This deviation is also responsible for significant deposition of sediments in the lateral moraine. A high variability in detrital SPDFs is also observed at a smaller spatial scale, when considering a similar approach of Enkelmann and Ehlers (2015), where sediments are collected upstream of the frontal moraine along a transverse transect (see supplementary materials): upstream. The trend of decreasing young age component in the detrital SPDF across the frontal moraine is seen for the AFT system, although the differences are less pronounced. However, this trend seems to be supported by a comparison with true ice-cored terminal moraine AFT data from Enkelmann and Ehlers (2015) (see A2). We observe that, from left to

right, the detrital age distributions within the frontal moraine incorporate older ages. However, we are aware that the method used to build SPDFs with a Gaussian kernel (Eq. 11) tends to break down with high (>30%) relative uncertainties (Brandon, 1996), as for the presented AFT data. We use this method for simplicity and to facilitate comparison with the synthetic AFT SPDFs. However, the original data also show the same tendency of age components getting older across the terminal moraine, and statistical tests applied on original data (Enkelmann and Ehlers, 2015) support the high variability of the detrital AFT age distributions across the terminal moraine regions (see Table A1). Overall, local sampling within the frontal moraine or upstream along a transverse transect leads to a higher variability in the inferred detrital age distributions. Even if some regions may show better agreement with the bedrock SPDF (region two), randomly sampling small patches of sediments through the moraine captures most of the age components on average and seems a better strategy overall.

#### 4.5 The effect of age uncertainties and age-elevation profiles: comparing AHe and AFT

The detrital AFT SPDFs for the previous model considering sampling on four regions within the frontal moraine share similar pattern (Fig. S9). Region one over-represents young ages (<25 Ma) and under-represents old ages (>25 Ma). Region two is like the bedrock SPDF, while region three and four tend to be biased toward older ages reflecting contributions from higher elevations. However, the variability between detrital AFT SPDF is much lower than for the detrital AHe SPDFs. Indeed, for all our models, we have seen that the behaviour of the mean detrital SPDFs from the AHe system differs from the AFT system. These differencesFor all of our models, we concluded that detrital age distributions resulting from the AFT ages were less informative than those from the AHe ages. The differences between the two systems occur for two main reasons. First, the age-elevation profiles differ. For the AFT profile, the youngest ages are not at the lowest elevation but occur at ~2000 m of elevation. The slope of the AFT age-elevation relationship is negative (but almost vertical (and actually negative) for elevations lower than 2000 m. This low age-elevation gradient leads to a reduction in source identifiability, i.e. similar ages can come from a large range of elevations. Secondly, the high relative age uncertainties (i.e. >30%) in the AFT data smooths the SPDF and decreases the resolvability of age components in the age distribution. Consequently, these two characteristics can make the AFT system perhaps less useful for tracking erosion patterns (Enkelmann and Ehlers, 2015; Ehlers et al., 2015), as seen for the case of non-uniform erosion. However, in some cases the AFT distribution can still capture first-order behaviour of sources if combined with bedrock age and age-elevation distributions, depending on the distribution of erosion across the catchment (Fig. S7i and Fig S9).

#### 5 ConclusionConclusions

In this study, we have modelledpresented a numerical approach to investigate the effect of erosion, sediment sources (hillslopes vs glaciers), ice transport and deposition on the distribution of thermochronological ages found in the frontal moraine of We applied this approach to a glaciated catchment which presents simple morphological characteristics: the Tiedemann glacier (British Columbia, Canada) in steady-state. Firstly, considering the kinematics of sediment particle transport reveals that

equilibrium, in the relative proportions of particles sources within the frontal moraine, is reached after 1500 yrs of ice transport. This result reflects the timescale of glacier dynamics and suggests that detrital SPDFs, in glaciated alpine catchments, are likely to reflect a transient case, especially for recent glacial deposits due for instance to glacier retreat. Secondly, the presence of small tributary glaciers, with very low velocities, may act as traps of ~~sediments~~ sediments and delay particle transfer to the glacier front. These low velocities may result from a morphodynamic feedback between the location of the ELA and the bed slope in direction of sliding. ~~Thirdly~~ Secondly, the transfer times of sediments are ~~not necessarily correlated~~ influenced by the proximity of their sources to the distance from the sampling site, as some ice streams showing high velocities. Indeed, sediments located in elevated areas may experience lower transfer times than sediments produced closer to the sampling site. ~~This effect is also linked to the presence of small tributary glaciers with low velocities, and to the~~ Thirdly, horizontal and vertical velocity distributions of the main glacier. Indeed, sources located at high elevations may deliver sediments directly to the centreline of the main glacier where the velocities are highest. ~~Fourthly, lateral spread~~ separation of ice flow lines may result in the deposition of ~~can produce~~ lateral moraines that may store a significant amount of ~~the sediments~~ sediment produced upstream. ~~Moreover, This implies that~~ frontal moraines may ~~have include~~ include sediments that contain thermochronological signatures from ~~only~~ limited parts of the total catchment, ~~leading to a potential bias in the estimation of age distributions.~~ To ~~limit~~ address this ~~issue~~ problem, lateral moraines of the same age deposition as the frontal moraine can be also targeted for complementary sampling, therefore incorporating more age components.

Sediment transport by ice can ~~introduces biases~~ lead to differences in the detrital age distributions compared to the bedrock age distribution, for instance by undersampling mid-~~altitudes~~ altitude age components. This could lead to misinterpretation of regional erosion patterns. ~~Therefore, an assessment of the spatial distribution of zones of low ice velocity, such as small tributary glaciers, and zones of intermediate storage of sediments may help to prevent such misinterpretation.~~ Moreover, ~~sampling~~ strategies considering local sampling of ~~sediments~~ sediment in the frontal moraine show variable detrital age distributions, that predominantly ~~reflects~~ reflect the variability of local sources upstream. In principle, this may allow us to directly associate particle sinks, e.g. moraines, to their sources. In contrast, randomly sampling through the frontal moraine potentially captures more age components, providing a more representative picture of the whole catchment. Therefore, we suggest ~~applying such a the~~ sampling strategy when possible. ~~However, we also emphasise the wide dispersion in detrital SPDFs that may result from sampling a limited amount of e.g. apatite grains (105 grains): should be designed according to the question being addressed.~~ Furthermore, we ~~have~~ systematically compared two thermochronological systems, AHe and AFT, with different but coherent age-elevation profiles and different relative age uncertainties. While the first factor plays a role in the ability to track sediment sources, the ~~latter decrease~~ second factor impacts on the precision of SPDFs ~~if high~~. However, characterization of the spatial variability of source contribution between different sampling sites may still be possible depending on the distribution of erosion.

Overall, ~~this study~~ your numerical approach offers novel insights on the application of detrital thermochronology to glaciated catchments and on the role of long-term exhumation, modern erosion, and past sediment transport. ~~Yet, our modelling approach neglects sediment transport by river and~~ However, as we have stated earlier, this study considers simple laws for ice motion

and sediment entrainment. ~~Future and neglects sediment transport by the glaciofluvial system. Clearly, directions for future studies should focus on~~ are the role of subglacial hydrology and ~~ice~~ plastic deformation of ice on sediment transport and ~~its associated detrital signal. Moreover on the role of meltwater in the building of terminal moraine. Finally, we have only considered one single alpine catchment and, our results may not apply~~ be applicable to larger ice systems, such as ice sheets.

5 ~~In particular, we have found that the detrital signal, recorded in the frontal moraine, reaches an equilibrium after  $10^3$  to  $10^4$  yrs, which is of the same order or lower than the periodicity of climatic signals during the Quaternary. In turn, the moraines of alpine glaciers may inform on the impact of this variability on catchment erosion. Moraines of larger ice sheets, which are likely associated to a larger range of sediment transfer times, may prove~~ catchments showing more informative—and also more challenging—to constrain erosion rates integrated over longer timescales and several climatic cycles. In particular, sediments

10 ~~deposited along the margins of the Antarctica and Greenland ice sheets represent good candidates to explore erosion rates over a time scale of  $10^5$  to  $10^6$  yr. complexity (e.g. tributary glacier valleys).~~

#### Author contribution

Maxime Bernard developed the model code for the computation of thermochronological ages and SPDFs, designed the experiments, and prepared the manuscript with contributions from Philippe Steer and Kerry Gallagher. David L. Egholm

15 provided the model iSOSIA with the associated knowledges to allow its use. He also contributed to the final version of the original draft.

#### Competing interest

The authors declare that they have no conflict of interest.

#### Acknowledgements

20 We thank Eva Enkelmann for having shared the AFT data from the Tiedemann glacier, which have been used to produce synthetic AFT ages. We also want to particularly thank the Insitut Français du Danemark (IFD) for having helped exchanges between Rennes and Aarhus with their financial support. Finally, we address special thanks to Peter Van der Beek, Stephane Bonnet, Benjamin Guillaume, and Pierre Valla, for their advices and guidance that ultimately conducted to this study.

#### Appendices

25 Table A1: Statistical tests results from Kuiper and Kolmogorov-Smirnov (KS) tests, with associated p-value for the modelled detrital CSPDFs shown in section 4.4. Each modelled detrital CSPDF (Region 1-4, and frontal moraine) is tested against the modelled catchment bedrock CSPDF. Frontal Moraine corresponds to the mean detrital CSPDF of the entire moraine. The variability of detrital SPDFs of the original data from Enkelmann and Ehlers (2015), p-values for S10-S14, has been tested by comparing the original ice-cored detrital SPDFs

against the detrital age distribution of the glacial outwash sample (9TETG15) presented in Ehlers et al. (2015). Highlighted in black are contradictions or p-value close to the alpha level (0.05) between the two statistical tests about the similarity between the corresponding detrital CSPDF and the catchment bedrock CSPDF (or glacial outwash in case of S10-S14). 1: the two distributions are different, 0: the two distributions are similar.

	AHe		AFT	
	Kuiper test/p-value	KS-test/p-value	Kuiper test/p-value	KS-test/p-value
Region 1	<u>1 / 1.16x10<sup>-5</sup></u>	<u>1 / 4.10x10<sup>-7</sup></u>	<u>1 / 1.37x10<sup>-6</sup></u>	<u>1 / 3.25.10<sup>-8</sup></u>
Region 2	<b>0 / 0.057</b>	<b>0 / 0.26</b>	<b>0 / 0.09</b>	<b>1 / 0.01</b>
Region 3	<u>1 / 1.63x10<sup>-9</sup></u>	<u>1 / 4.80x10<sup>-8</sup></u>	<b>1 / 6.42x10<sup>-22</sup></b>	<u>1 / 3.26x10<sup>-24</sup></u>
Region 4	<u>1 / 4.46x10<sup>-11</sup></u>	<b>1 / 4.68x10<sup>-9</sup></b>	<u>1 / 5.78x10<sup>-20</sup></u>	<u>1 / 3.38x10<sup>-22</sup></u>
Frontal Moraine	<b>0 / 0.50</b>	<b>0 / 0.55</b>	<u>0 / 0.87</u>	<u>0 / 0.31</u>
S10	=	=	<u>1 / 8.83x10<sup>-16</sup></u>	<u>1 / 1.30x10<sup>-17</sup></u>
S11	=	=	<u>1 / 4.99x10<sup>-9</sup></u>	<u>1 / 4.03x10<sup>-7</sup></u>
S12	=	=	<b>1 / 0.03</b>	<b>0 / 0.30</b>
S13	=	=	<u>0 / 0.25</u>	<u>0 / 0.38</u>
S14	=	=	<u>0 / 0.52</u>	<u>0 / 0.10</u>

### Code availability

The iSOSIA version (iSOSIA\_3.4.7b) and the external routine used to compute the detrital age distributions are publicly available here: <https://github.com/davidlundbek/iSOSIA>.

### 5 References

Anderson, R. S.: Evolution of lumpy glacial landscapes. *Geology*, 42(8), 679–682, 2014.

Avdeev, B., Niemi, N. A., and Clark, M. K.: Doing more with less: Bayesian estimation of erosion models with detrital thermochronometric data. *Earth and Planetary Science Letters*, 305(3–4), 385–395, 2011.

10 Alley, R. B., Cuffey, K. M., Evenson, E. B., Strasser, J. C., Lawson, D. E., and Larson, G. J.: How glaciers entrain and transport basal sediment: physical constraints. *Quaternary Science Reviews*, 16(9), 1017–1038, 1997. [https://doi.org/10.1016/S0277-3791\(97\)00034-6](https://doi.org/10.1016/S0277-3791(97)00034-6), 1997.

Anderson, R. S.: Evolution of lumpy glacial landscapes. *Geology*, 42(8), 679–682. <https://doi.org/10.1130/G35537.1>, 2014.

Mis en forme : Couleur de police : Automatique

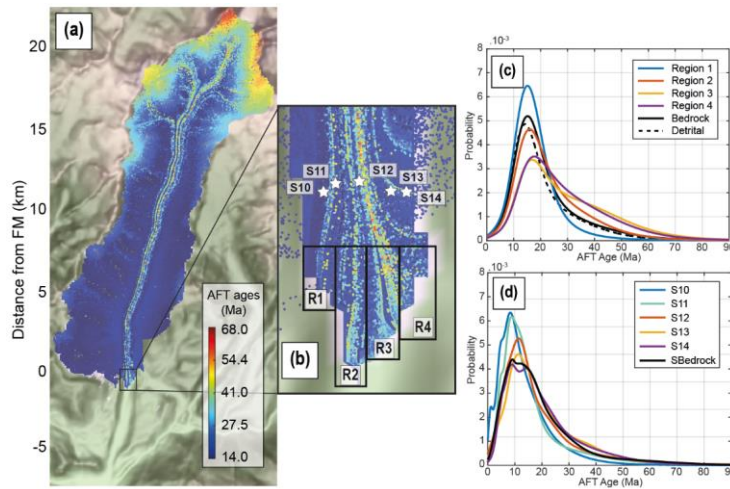


**Figure A2:** Detrital AFT age distributions of the four regions seen in (b, black rectangles) from the experiment considering uniform source of particles (a). The density plots of modelled detrital AFT ages are shown in (c). The dashed black line is the mean detrital SPDF for the frontal moraine (FM). The ice-cored detrital SPDFs from Enkelmann and Ehlers (2015), is shown in (d). Each sample (S10–14) is located in (b) by the white stars, and the age distributions have been built using the method explained in Sect. 2.4. The bedrock SPDF in (d) results from the bedrock single grain age distribution presented in Enkelmann and Ehlers (2015).

Avdeev, B., Niemi, N. A., and Clark, M. K.: Doing more with less: Bayesian estimation of erosion models with detrital thermochronometric data. *Earth and Planetary Science Letters*, 305(3-4), 385-395, <https://doi.org/10.1016/j.epsl.2011.03.020>, 2011.

Beaumont, C., Fullsack, P., and Hamilton, J.: Erosional control of active compressional orogens. In *Thrust tectonics* (pp. 1-18). Springer, Dordrecht, 1992.

Benn, D., and Evans, D. J.: *Glaciers and glaciation*. Routledge, second edition, New York, USA, 2013.

Bernard, T., Steer, P., Gallagher, K., Szulc, A., Whitham, A., & Johnson, C.: Evidence for Eocene–Oligocene glaciation in the landscape of the East Greenland margin. *Geology*, 44(11), 895-898, 2016. <https://doi.org/10.1130/G38248.1>, 2016.

Boulton G.S.: Processes and Patterns of Glacial Erosion. In: Coates D.R. (eds) *Glacial Geomorphology*. Springer, Dordrecht, 1982.

Bowman, D., Eyles, C. H., Narro-Pérez, R., and Vargas, R.: Sedimentology and Structure of the Lake Palcacocha Laterofrontal Moraine Complex in the Cordillera Blanca, Peru. *Revista de Glaciares y Ecosistemas de Montaña*, (5), 16-16, <https://doi.org/10.36580/rgem.i5.27-42>, 2018.

Brædstrup, C. F., Egholm, D. L., Ugelvig, S. V., and Pedersen, V. K.: Basal shear stress under alpine glaciers: insights from experiments using the iSOSIA and Elmer/Ice models. *Earth Surface Dynamics*, 4(1), 2016. <https://doi.org/10.5194/esurf-4-159-2016>, 2016.

Brandon, M. T.: Probability density plot for fission-track grain-age samples. *Radiation Measurements*, 26(5), 663-676, 1996. [https://doi.org/10.1016/S1350-4487\(97\)82880-6](https://doi.org/10.1016/S1350-4487(97)82880-6), 1996.

Brewer, I. D., Burbank, D. W., and Hodges, K. V.: Modelling detrital cooling-age populations: insights from two Himalayan catchments. *Basin Research*, 15(3), 305-320, 2003. <https://doi.org/10.1046/j.1365-2117.2003.00211.x>, 2003.

Brozović, N., Burbank, D. W., and Meigs, A. J.: Climatic limits on landscape development in the northwestern Himalaya. *Science*, 276(5312), 571-574, <https://doi.org/10.1126/science.276.5312.571>, 1997.

Champagnac, J. D., Valla, P. G., and Herman, F.: Late-Cenozoic relief evolution under evolving climate: A review. *Tectonophysics*, 614, 44-65, <https://doi.org/10.1016/j.tecto.2013.11.037>, 2014.

Clarke, G. K.: A short history of scientific investigations on glaciers. *Journal of Glaciology*, 33(S1), 4-24, <https://doi.org/10.3189/S0022143000215785>, 1987.

Cohen, D., Iverson, N. R., Hooyer, T. S., Fischer, U. H., Jackson, M., and Moore, P. L.: Debris-bed friction of hard-bedded glaciers. *Journal of Geophysical Research: Earth Surface*, 110(F2), 2005. <https://doi.org/10.1029/2004JF000228>, 2005.

Cohen, D., Hooyer, T. S., Iverson, N. R., Thomason, J. F., and Jackson, M.: Role of transient water pressure in quarrying: A subglacial experiment using acoustic emissions. *Journal of Geophysical Research: Earth Surface*, 111(F3), 2006. <https://doi.org/10.1029/2005JF000439>, 2006.

Collins, D. N.: Sediment transport from glacierized basins in the. In *Erosion and Sediment Yield: Global and Regional Perspectives: Proceedings of an International Symposium Held at Exeter, UK, from 15 to 19 July 1996* (No. 236, p. 85). IAHS, <https://doi.org/10.3389/feart.2018.00175>, 1996.

Mis en forme : Couleur de police : Automatique

Mis en forme : Couleur de police : Automatique

Mis en forme : Couleur de police : Automatique

Mis en forme : Couleur de police : Automatique

Mis en forme : Couleur de police : Automatique

Mis en forme : Couleur de police : Automatique

Mis en forme : Couleur de police : Automatique, Motif : Transparente

- Delaney, I., Bauder, A., Werder, M. A., and Farinotti, D.: Regional and annual variability in subglacial sediment transport by water for two glaciers in the Swiss Alps. *Frontiers in Earth Science*, 6, 175, <https://doi.org/10.3389/feart.2018.00175>, 2018.
- Egholm, D., Bernard, M.: iSOSIA\_3.4.7b, Zenodo, <https://doi.org/10.5281/zenodo.3875297>, 2020.
- 5 Egholm, D. L., Knudsen, M. F., Clark, C. D., and Lesemann, J. E.: Modeling the flow of glaciers in steep terrains: The integrated second-order shallow ice approximation (iSOSIA). *Journal of Geophysical Research: Earth Surface*, 116(F2), 2011, <https://doi.org/10.1029/2010JF001900>, 2011.
- Egholm, D. L., Nielsen, S., Pedersen, V. K., and Lesemann, J.E: Glacial effects limiting mountain height, *Nature*, 460(7257), 884–887, 2009, <https://doi.org/10.1038/nature08263>, 2009.
- Egholm, D. L., Pedersen, V. K., Knudsen, M. F., and Larsen, N. K.: Coupling the flow of ice, water, and sediment in a glacial landscape evolution model. *Geomorphology*, 141, 47-66, <https://doi.org/10.1016/j.geomorph.2011.12.019>, 2012a.
- 10 Egholm, D. L., Pedersen, V. K., Knudsen, M. F., and Larsen, N. K.: On the importance of higher order ice dynamics for glacial landscape evolution. *Geomorphology*, 141, 67-80, <https://doi.org/10.1016/j.geomorph.2011.12.020>, 2012b.
- Ehlers, T. A.: Crustal thermal processes and the interpretation of thermochronometer data. *Reviews in Mineralogy and Geochemistry*, 58(1), 315-350, 2005, <https://doi.org/10.2138/rmg.2005.58.12>, 2005.
- 15 Ehlers, T. A., Szameitat, A., Enkelmann, E., Yanites, B. J., and Woodsworth, G. J.: Identifying spatial variations in glacial catchment erosion with detrital thermochronology. *Journal of Geophysical Research: Earth Surface*, 120(6), 1023-1039, 2015, <https://doi.org/10.1002/2014JF003432>, 2015.
- Enkelmann, E., and Ehlers, T. A.: Evaluation of detrital thermochronology for quantification of glacial catchment denudation and sediment mixing. *Chemical Geology*, 411, 299-309, 2015, <https://doi.org/10.1016/j.chemgeo.2015.07.018>, 2015.
- 20 Enkelmann, E., Zeitler, P. K., Pavlis, T. L., Garver, J. I., and Ridgway, K. D.: Intense localized rock uplift and erosion in the St Elias orogen of Alaska. *Nat. Geosci.* 2 (5), 360–363, 2009, <https://doi.org/10.1038/ngeo502>, 2009.
- Ewertowski, M. W., and Tomczyk, A. M.: Reactivation of temporarily stabilized ice-cored moraines in front of polythermal glaciers: Gravitational mass movements as the most important geomorphological agents for the redistribution of sediments (a case study from Ebbabreen and Ragnarbreen, Svalbard). *Geomorphology*, 350, <https://doi.org/10.1016/j.geomorph.2019.106952>, 2020.
- 25 Falkowski, S., Enkelmann, E., Drost, K., Pfänder, J. A., Stübner, K., and Ehlers, T. A.: Cooling history of the St. Elias syntaxis, southeast Alaska, revealed by geochronology and thermochronology of cobble-sized glacial detritus. *Tectonics*, 35(2), 447-468, 2016, <https://doi.org/10.1002/2015TC004086>, 2016.
- Farinotti, D., Brinkerhoff, D., Clarke, G. K., Fürst, J. J., Frey, H., Gantayat, P., ... and Linsbauer, A.: How accurate are estimates of glacier ice thickness? Results from ITMIX, the Ice Thickness Models Intercomparison eXperiment. *The Cryosphere Discussions*, 2016, <https://doi.org/10.5194/tc-2016-250>, 2016.
- 30 Farinotti, D., Huss, M., Fürst, J. J., Landmann, J., Machguth, H., Maussion, F., and Pandit, A.: A consensus estimates for the ice thickness distribution of all glaciers on Earth. *Nature Geoscience*, 12(3), 168, 2019, <https://doi.org/10.1038/s41561-019-0300-3>, 2019.

Mis en forme : Couleur de police : Automatique, Motif : Transparente

Mis en forme : Couleur de police : Automatique

Mis en forme : Couleur de police : Automatique

Mis en forme : Police :Gras

Mis en forme : Couleur de police : Automatique

Mis en forme : Couleur de police : Automatique, Motif : Transparente

Mis en forme : Couleur de police : Automatique

Mis en forme : Couleur de police : Automatique

- Farley, K. A., and Stockli, D. F.: (U-Th)/He dating of phosphates: Apatite, monazite, and xenotime. *Reviews in mineralogy and geochemistry*, 48(1), 559-577, [2002-https://doi.org/10.2138/rmg.2002.48.15](https://doi.org/10.2138/rmg.2002.48.15), 2002.
- Fitzgerald, P. G., and Stump, E.: Cretaceous and Cenozoic episodic denudation of the Transantarctic Mountains, Antarctica: New constraints from apatite fission track thermochronology in the Scott Glacier region. *Journal of Geophysical Research: Solid Earth*, 102(B4), 7747-7765, <https://doi.org/10.1029/96JB03898>, 1997.
- Galbraith, R. F.: *Statistics for fission track analysis*. Chapman and Hall/CRC, 2005.
- Gallagher, K.: Evolving temperature histories from apatite fission-track data. *Earth and Planetary Science Letters*, 136(3-4), 421-435, [https://doi.org/10.1016/0012-821X\(95\)00197-K](https://doi.org/10.1016/0012-821X(95)00197-K), 1995.
- Gallagher, K., and Parra, M.: A new approach to thermal history modelling with detrital low temperature thermochronological data. *Earth and Planetary Science Letters*, 529, 115872, [2020-https://doi.org/10.1016/j.epsl.2019.115872](https://doi.org/10.1016/j.epsl.2019.115872), 2020.
- Glen, J. W.: Experiments on the deformation of ice. *Journal of Glaciology*, 2(12), 111-114, <https://doi.org/10.3189/S0022143000034067>, 1952.
- Glotzbach, C., Busschers, F. S., and Winsemann, J.: Detrital thermochronology of Rhine, Elbe and Meuse river sediment (Central Europe): implications for provenance, erosion and mineral fertility. *International Journal of Earth Sciences*, 107(2), 459-479, [2018-https://doi.org/10.1007/s00531-017-1502-9](https://doi.org/10.1007/s00531-017-1502-9), 2018.
- Godon, C., Mugnier, J. L., Fallourd, R., Paquette, J. L., Pohl, A., and Buoncristiani, J. F.: The Bossons glacier protects Europe's summit from erosion. *Earth and Planetary Science Letters*, 375, 135-147, <https://doi.org/10.1016/j.epsl.2013.05.018>, 2013.
- Goodsell, B., Hambrey, M. J., and Glasser, N. F.: Debris transport in a temperate valley glacier: Haut Glacier d'Arolla, Valais, Switzerland. *Journal of Glaciology*, 51(172), 139-146, [2005-https://doi.org/10.3189/172756505781829647](https://doi.org/10.3189/172756505781829647), 2005.
- Grabowski, D. M., Enkelmann, E., and Ehlers, T. A.: Spatial extent of rapid denudation in the glaciated St. Elias syntaxis region, SE Alaska. *Journal of Geophysical Research: Earth Surface*, 118(3), 1921-1938, [2013-https://doi.org/10.1002/jgrf.20136](https://doi.org/10.1002/jgrf.20136), 2013.
- Guillon, H., Mugnier, J. L., Buoncristiani, J. F., Carcaillet, J., Godon, C., Prud'Homme, C., Van der Beek, P., and Vassallo, R.: Improved discrimination of subglacial and periglacial erosion using  $^{10}\text{Be}$  concentration measurements in subglacial and supraglacial sediment load of the Bossons glacier (Mont Blanc massif, France). *Earth Surface Processes and Landforms*, 40(9), 1202-1215, <https://doi.org/10.1002/esp.3713>, 2015.
- Hallet, B.: Subglacial regelation water film. *Journal of Glaciology*, 23(89), 321-334, <https://doi.org/10.3189/S0022143000029932>, 1979.
- Hallet, B.: Glacial abrasion and sliding: their dependence on the debris concentration in basal ice. *Annals of Glaciology*, 2, 23-28, <https://doi.org/10.3189/172756481794352487>, 1981.
- Hallet, B., Hunter, L., and Bogen, J.: Rates of erosion and sediment evacuation by glaciers: A review of field data and their implications. *Global and Planetary Change*, 12(1-4), 213-235, 1996.
- Hambrey, M. J., Bennett, M. R., Dowdeswell, J. A., Glasser, N. F., and Huddart, D.: Debris entrainment and transfer in polythermal valley glaciers. *Journal of Glaciology*, 45(149), 69-86, <https://doi.org/10.3189/S0022143000003051>, 1999.

Mis en forme : Couleur de police : Automatique

Mis en forme : Couleur de police : Automatique

Mis en forme : Couleur de police : Automatique, Motif : Transparente

Mis en forme : Couleur de police : Automatique

Mis en forme : Couleur de police : Automatique

Mis en forme : Couleur de police : Automatique

Mis en forme : Couleur de police : Automatique

Mis en forme : Couleur de police : Automatique

Mis en forme : Couleur de police : Automatique

Mis en forme : Couleur de police : Automatique

Mis en forme : Couleur de police : Automatique

Mis en forme : Couleur de police : Automatique

- Hambrey, M. J., and Lawson, W.: Structural styles and deformation fields in glaciers: a review. Geological Society, London, Special Publications, 176(1), 59-83, 2000-<https://doi.org/10.1144/GSL.SP.2000.176.01.06>, 2000.
- Hambrey, M. J., Quincey, D. J., Glasser, N. F., Reynolds, J. M., Richardson, S. J., and Clemmens, S.: Sedimentological, geomorphological and dynamic context of debris-mantled glaciers, Mount Everest (Sagarmatha) region, Nepal. *Quaternary Science Reviews*, 27(25-26), 2361-2389, <https://doi.org/10.1016/j.quascirev.2008.08.010>, 2008.
- Herman, F., Beaud, F., Champagnac, J. D., Lemieux, J. M., and Sternai P.: Glacial hydrology and erosion patterns: A mechanism for carving glacial valleys, *Earth Planet. Sci. Lett.*, 310(3), 498-508, 2011-<https://doi.org/10.1016/j.epsl.2011.08.022>, 2011.
- Herman, F., Braun, J., Deal, E., and Prasicsek, G.: The response time of glacial erosion. *Journal of Geophysical Research: Earth Surface*, 123(4), 801-817, <https://doi.org/10.1002/2017JF004586>, 2018.
- Herman, F., Seward, D., Valla, P. G., Carter, A., Kohn, B., Willett, S. D., and Ehlers, T. A.: Worldwide acceleration of mountain erosion under a cooling climate. *Nature*, 504(7480), 423, 2013-<https://doi.org/10.1038/nature12877>, 2013.
- Hindmarsh, R. C.: The role of membrane-like stresses in determining the stability and sensitivity of the Antarctic ice sheets: back pressure and grounding line motion. *Philosophical Transactions of the Royal Society A: Mathematical, Physical and Engineering Sciences*, 364(1844), 1733-1767, 2006-<https://doi.org/10.1098/rsta.2006.1797>, 2006.
- Hurford, A. J., and Green, P. F.: The zeta age calibration of fission-track dating. *Chemical Geology*, 41, 285-317, [https://doi.org/10.1016/S0009-2541\(83\)80026-6](https://doi.org/10.1016/S0009-2541(83)80026-6), 1983.
- Iverson, N. R.: A theory of glacial quarrying for landscape evolution models. *Geology*, 40(8), 679-682, 2012-<https://doi.org/10.1130/G33079.1>, 2012.
- Iverson, N. R., Cohen, D., Hooyer, T. S., Fischer, U. H., Jackson, M., Moore, P. L., ... and Kohler, J.: Effects of basal debris on glacier flow. *Science*, 301(5629), 81-84, 2003-<https://doi.org/10.1126/science.1083086>, 2003.
- Jarvis, A., Reuter, R.I., Nelson, A., Guevara E.: Hole-filled seamless SRTM data V4, International Centre for Tropical Agriculture (CIAT), available from <http://srtm.csi.cgiar.org>, 2008.
- Jóhannesson, T., Raymond, C. F., and Waddington, E. D.: A simple method for determining the response time of glaciers. *In Glacier fluctuations and climatic change (pp. 343-352)*. Springer, Dordrecht, [https://doi.org/10.1007/978-94-015-7823-3\\_22](https://doi.org/10.1007/978-94-015-7823-3_22), 1989.
- Kayastha, R. B., Takeuchi, Y., Nakawo, M., and Ageta, Y.: Practical prediction of ice melting beneath various thickness of debris cover on Khumbu Glacier, Nepal, using a positive degree-day factor, *IAHS-AISH P*, 264, 71-81, 2000.
- Kessler, M. A., Anderson, R. S., and Briner J. P.: Fjord insertion into continental margins driven by topographic steering of ice, *Nat.Geosci.*, 1(6), 365-369, 2008-<https://doi.org/10.1038/ngeo201>, 2008.
- Kirkbride, M. P.: Processes of glacial transportation. In *Modern and Past Glacial Environments (pp. 147-169)*. Butterworth-Heinemann, 2002-<https://doi.org/10.1016/B978-075064226-2/50009-X>, 2002.
- Koppes, M., Hallet, B., Rignot, E., Mouginot, J., Wellner, J. S., and Boldt, K.: Observed latitudinal variations in erosion as a function of glacier dynamics. *Nature*, 526(7571), 100, 2015-<https://doi.org/10.1038/nature15385>, 2015.

Mis en forme : Couleur de police : Automatique

Mis en forme : Couleur de police : Automatique

Mis en forme : Couleur de police : Automatique

Mis en forme : Couleur de police : Automatique

Mis en forme : Couleur de police : Automatique

Mis en forme : Couleur de police : Automatique

Mis en forme : Couleur de police : Automatique

Mis en forme : Couleur de police : Automatique

Mis en forme : Couleur de police : Automatique

- Koppes, M. N., and Montgomery, D. R.: The relative efficacy of fluvial and glacial erosion over modern to orogenic timescales. *Nature Geoscience*, 2(9), 644, 2009-<https://doi.org/10.1038/ngeo616>, 2009.
- Lukas, S.: A test of the englacial thrusting hypothesis of 'hummocky' moraine formation: case studies from the northwest Highlands, Scotland. *Boreas*, 34(3), 287-307, <https://doi.org/10.1111/j.1502-3885.2005.tb01102.x>, 2005.
- 5 Matsuoka, N., Murton, J.: Frost weathering: recent advances and future directions. *Permafrost and Periglacial Processes*, 19(2), 195-210, 2008, <https://doi.org/10.1002/ppp.620>, 2008.
- MacGregor, K. C., Anderson, R. S., Anderson, S. P., and Waddington, E. D.: Numerical simulations of longitudinal profile evolution of glacial valleys, *Geology* 28 (11): 1031-1034, 2000-[https://doi.org/10.1130/0091-7613\(2000\)28<1031:NSOGLP>2.0.CO;2](https://doi.org/10.1130/0091-7613(2000)28<1031:NSOGLP>2.0.CO;2), 2000.
- 10 MacGregor, K. R., Anderson, R. S., and Waddington, E. D.: Numerical modelling of glacial erosion and headwall processes in alpine valleys. *Geomorphology*, 103(2), 189-204, <https://doi.org/10.1016/j.geomorph.2008.04.022>, 2009.
- Menounos, B., Clague, J. J., Clarke, G. K., Marcott, S. A., Osborn, G., Clark, P. U., Tennant C., and Novak, A. M.: Did rock avalanche deposits modulate the late Holocene advance of Tiedemann Glacier, southern Coast Mountains, British Columbia, Canada?. *Earth and Planetary Science Letters*, 384, 154-164, <https://doi.org/10.1016/j.epsl.2013.10.008>, 2013.
- 15 Moecher, D. P., and Samson, S. D.: Differential zircon fertility of source terranes and natural bias in the detrital zircon record: Implications for sedimentary provenance analysis. *Earth and Planetary Science Letters*, 247(3-4), 252-266, <https://doi.org/10.1016/j.epsl.2006.04.035>, 2006.
- Molnar, P., and England, P.: Late Cenozoic uplift of mountain ranges and global climate change: chicken or egg?. *Nature*, 346(6279), 29, <https://doi.org/10.1038/346029a0>, 1990.
- 20 Montgomery, D. R., and Brandon, M. T.: Topographic controls on erosion rates in tectonically active mountain ranges. *Earth and Planetary Science Letters*, 201(3-4), 481-489, 2002-[https://doi.org/10.1016/S0012-821X\(02\)00725-2](https://doi.org/10.1016/S0012-821X(02)00725-2), 2002.
- Nussbaumer, S., Zumbühl, H. J., and Steiner, D.: Fluctuations of the Mer de Glace (Mont Blanc area, France) AD 1500-2050: An interdisciplinary approach using new historical data and neural network simulations. *Zeitschrift für Gletscherkunde und Glazialgeologie ZGG*, (40), 5-175, 2007.
- 25 Osborn, G., and Luckman, B. H.: Holocene glacier fluctuations in the Canadian cordillera (Alberta and British Columbia). *Quaternary Science Reviews*, 7(2), 115-128, 1988.
- Oerlemans, J.: *Glaciers and climate change*. CRC Press, 2001.
- Östrem, G.: Ice melting under a thin layer of moraine, and the existence of ice cores in moraine ridges. *Geografiska Annaler*, 41(4), 228-230, 1959-<https://doi.org/10.1080/20014422.1959.11907953>, 1959.
- 30 Roe, G. H., and O'Neal, M. A.: The response of glaciers to intrinsic climate variability: observations and models of late-Holocene variations in the Pacific Northwest. *Journal of Glaciology*, 55(193), 839-854, <https://doi.org/10.3189/002214309790152438>, 2009.

Mis en forme : Couleur de police : Automatique

Mis en forme : Couleur de police : Automatique

Mis en forme : Couleur de police : Automatique

Mis en forme : Couleur de police : Automatique

Mis en forme : Couleur de police : Automatique

- Roering, J. J., Kirchner, J. W., and Dietrich, W. E.: Evidence for nonlinear, diffusive sediment transport on hillslopes and implications for landscape morphology. *Water Resources Research*, 35(3), 853-870, <https://doi.org/10.1029/1998WR900090>, 1999.
- 5 Rowan, A. V., Egholm, D. L., Quincey, D. J., and Glasser, N. F.: Modelling the feedbacks between mass balance, ice flow and debris transport to predict the response to climate change of debris-covered glaciers in the Himalaya. *Earth and Planetary Science Letters*, 430, 427-438, 2015-<https://doi.org/10.1016/j.epsl.2015.09.004>, 2015.
- Ruhl, K. W., and Hodges, K. V.: The use of detrital mineral cooling ages to evaluate steady state assumptions in active orogens: An example from the central Nepalese Himalaya. *Tectonics*, 24(4), 2005-<https://doi.org/10.1029/2004TC001712>, 2005.
- Schildgen, T. F., Van der Beek, P. A., Sinclair, H. D., and Thiede, R. C.: Spatial correlation bias in late-Cenozoic erosion histories derived from thermochronology. *Nature*, 559(7712), 89, 2018-<https://doi.org/10.1038/s41586-018-0260-6>, 2018.
- 10 Schoof, C.: The effect of cavitation on glacier sliding. *Proceedings of the Royal Society A: Mathematical, Physical and Engineering Sciences*, 461(2055), 609-627, 2005-<https://doi.org/10.1098/rspa.2004.1350>, 2005.
- Schoof, C.: Ice-sheet acceleration driven by melt supply variability. *Nature*, 468(7325), 803, 2010-<https://doi.org/10.1038/nature09618>, 2010.
- 15 Sharp, M.: Annual moraine ridges at Skálafellsjökull, south-east Iceland. *Journal of Glaciology*, 30(104), 82-93, <https://doi.org/10.3189/S0022143000008522>, 1984.
- Small, R. J.: Englacial and supraglacial sediment: transport and deposition. In Gurnell, A.M. and Clark, M.J. (eds), *Glacio-Fluvial Sediment Transfer: An Alpine Perspective*. Wiley, Chichester, 111-45, 1987.
- Spedding, N. I. C. K.: Hydrological controls on sediment transport pathways: implications for debris-covered glaciers. IAHS publication, 133-142, 2000.
- 20 Steer, P., Huisman, R. S., Valla, P. G., Gac, S., & Herman, F.: Bimodal Plio–Quaternary glacial erosion of fjords and low-relief surfaces in Scandinavia. *Nature Geoscience*, 5(9), 635-639, 2012-<https://doi.org/10.1038/ngeo1549>, 2012.
- Stock, G. M., Ehlers, T. A., and Farley, K. A.: Where does sediment come from? Quantifying catchment erosion with detrital apatite (U-Th)/He thermochronometry. *Geology*, 34(9), 725-728, 2006-<https://doi.org/10.1130/G22592.1>, 2006.
- 25 [Swift, D. A., Nienow, P. W., and Hoey, T. B.: Basal sediment evacuation by subglacial meltwater: suspended sediment transport from Haut Glacier d'Arolla, Switzerland. \*Earth Surface Processes and Landforms\*, 30\(7\), 867-883, <https://doi.org/10.1002/esp.1197>, 2005.](https://doi.org/10.1002/esp.1197)
- 30 [Tennant, C., Menounos, B., Ainslie, B., Shea, J., and Jackson, P.: Comparison of modeled and geodetically-derived glacier mass balance for Tiedemann and Klinaklini glaciers, southern Coast Mountains, British Columbia, Canada. \*Global and planetary change\*, 82, 74-85, <https://doi.org/10.1016/j.gloplacha.2011.11.004>, 2012.](https://doi.org/10.1016/j.gloplacha.2011.11.004)
- Thomson, S. N., Reiners, P. W., Hemming, S. R., and Gehrels, G. E.: The contribution of glacial erosion to shaping the hidden landscape of East Antarctica. *Nature Geoscience*, 6(3), 203, 2013-<https://doi.org/10.1038/ngeo1722>, 2013.

Mis en forme : Couleur de police : Automatique

Mis en forme : Couleur de police : Automatique, Motif : Transparente

Mis en forme : Couleur de police : Automatique, Motif : Transparente

Mis en forme : Couleur de police : Automatique

Mis en forme : Couleur de police : Automatique

Mis en forme : Couleur de police : Automatique

Mis en forme : Couleur de police : Automatique

Mis en forme : Couleur de police : Automatique

Mis en forme : Police :Gras, Couleur de police : Automatique, Motif : Transparente

Mis en forme : Couleur de police : Automatique

- Tranel, L. M., Spotila, J. A., Kowalewski, M. J., and Waller, C. M.: Spatial variation of erosion in a small, glaciated basin in the Teton Range, Wyoming, based on detrital apatite (U-Th)/He thermochronology. *Basin Research*, 23(5), 571-590, 2011. <https://doi.org/10.1111/j.1365-2117.2011.00502.x>, 2011.
- Ugelvig, S. V., Egholm, D. L., Anderson, R. S., and Iverson, N. R.: Glacial Erosion Driven by Variations in Meltwater Drainage. *Journal of Geophysical Research: Earth Surface*, 123(11), 2863-2877, 2018. <https://doi.org/10.1029/2018JF004680>, 2018.
- Ugelvig, S. V., Egholm, D. L., and Iverson, N. R.: Glacial landscape evolution by subglacial quarrying: A multiscale computational approach. *Journal of Geophysical Research: Earth Surface*, 121(11), 2042-2068, 2016. <https://doi.org/10.1002/2016JF003960>, 2016.
- Valla, P. G., Van der Beek, P. A., and Braun, J.: Rethinking low-temperature thermochronology data sampling strategies for quantification of denudation and relief histories: a case study in the French western Alps. *Earth and Planetary Science Letters*, 307(3-4), 309-322, <https://doi.org/10.1016/j.epsl.2011.05.003>, 2011a.
- Valla, P. G., Shuster, D. L., and Van Der Beek, P. A.: Significant increase in relief of the European Alps during mid-Pleistocene glaciations. *Nature Geoscience*, 4(10), 688, <https://doi.org/10.1038/ngeo1242>, 2011b.
- Vermeesch, P.: How many grains are needed for a provenance study?. *Earth and Planetary Science Letters*, 224(3-4), 441-451, 2004. <https://doi.org/10.1016/j.epsl.2004.05.037>, 2004.
- Whipple, K. X.: The influence of climate on the tectonic evolution of mountain belts. *Nature geoscience*, 2(2), 97, 2009. <https://doi.org/10.1038/ngeo413>, 2009.
- Willenbring, J. K., and Jerolmack, D. J.: The null hypothesis: globally steady rates of erosion, weathering fluxes and shelf sediment accumulation during Late Cenozoic mountain uplift and glaciation. *Terra Nova*, 28(1), 11-18, 2016. <https://doi.org/10.1111/ter.12185>, 2016.
- Winkler, S., and Matthews, J. A.: Observations on terminal moraine-ridge formation during recent advances of southern Norwegian glaciers. *Geomorphology*, 116(1-2), 87-106, <https://doi.org/10.1016/j.geomorph.2009.10.011>, 2010.
- Yanites, B. J., and Ehlers, T. A.: Intermittent glacial sliding velocities explain variations in long-timescale denudation. *Earth and Planetary Science Letters*, 450, 52-61, <https://doi.org/10.1016/j.epsl.2016.06.022>, 2016.
- Zachos, J., Pagani, M., Sloan, L., Thomas, E., and Billups, K.: Trends, rhythms, and aberrations in global climate 65 Ma to present. *science*, 292(5517), 686-693, 2001. <https://doi.org/10.1126/science.1059412>, 2001.

Mis en forme : Couleur de police : Automatique

Mis en forme : Couleur de police : Automatique

Mis en forme : Couleur de police : Automatique

Mis en forme : Couleur de police : Automatique

Mis en forme : Couleur de police : Automatique

Mis en forme : Couleur de police : Automatique

Mis en forme : Couleur de police : Automatique

Mis en forme : Couleur de police : Automatique, Motif : Transparente